DISCLAIMER

This report was prepared as an account of work sponsored by an agency of the United States Government. Neither the United States Government nor any agency thereof, nor any of their employees, makes any warranty, express or implied, or assumes any legal liability or responsibility for the accuracy, completeness, or usefulness of any information, apparatus, product, or process disclosed, or represents that its use would not infringe privately owned rights. Reference herein to any specific commercial product, process, or service by trade name, trademark, manufacturer, or otherwise does not necessarily constitute or imply its endorsement, recommendation, or favoring by the United States Government or any agency thereof. The views and opinions of authors expressed herein do not necessarily state or reflect those of the United States Government or any agency thereof. Reference herein to any social initiative (including but not limited to Diversity, Equity, and Inclusion (DEI); Community Benefits Plans (CBP); Justice 40; etc.) is made by the Author independent of any current requirement by the United States Government and does not constitute or imply endorsement, recommendation, or support by the United States Government or any agency thereof.

CASL-U-2017-4148-000

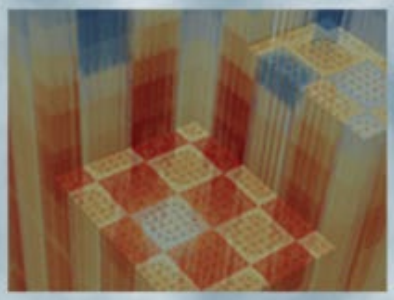

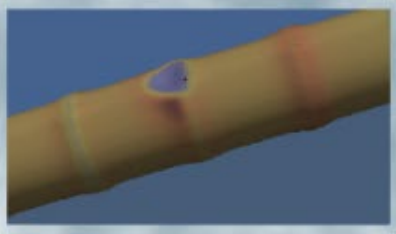

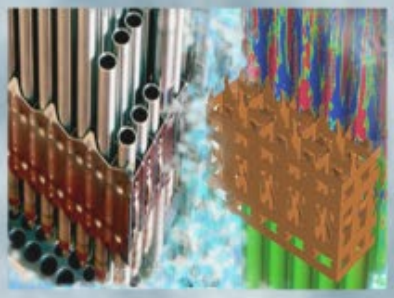

VERA Core Physics Benchmark Progression Problem Results for VERA 3.6

Nathan Andrews, Sandia National Laboratories
Natalie Gordon, Sandia National Laboratories
Andrew Godfrey, Oak Ridge National Laboratory

April 27, 2017

REVISION LOG

Revision	Date	Affected Pages	Revision Description
0	4/27/2017	All	Initial Release

Document pages that are:

Export Controlled N/A

IP/Proprietary/NDA Controlled N/A

Sensitive Controlled N/A

Requested Distribution:

To: N/A

Copy: N/A

EXECUTIVE SUMMARY

This report contains a comparison of results obtained with VERA 3.6 Release Candidate 0 for the Core Physics Benchmark Progression Problems 1 through 9 to both computational tools and measured data from Watts Bar Unit 1 (WBN1). (Ref. 1 and Ref. 2) These problems progress from single pin cell analyses to full core depletion calculations.

VERA results obtained for Problems 1 through 5 are compared against results obtained using the SCALE 6.2 Beta code KENO-VI. Results for Problem 6 and 7 are compared against those obtained using a coupled neutronic and thermal-hydraulic combination of the KAPL software MC21 and the CASL tool CTF. (Ref. 3, Ref. 4 and Ref. 5) VERA results from problems 5and 9 are compared to data from WBN1.

For all of the analyses contained in this report, VERA provided similar results to other state-of-the-art software programs and real reactor data. This indicates that the program is capable of modeling a full-scale PWR in a more discretized and computationally efficient manner than any other reactor physics program.

Since the descriptions of the Core Physics Benchmark Progression Problems and the logic behind their selection is discussed in-depth elsewhere it is not covered in the scope of this document. Additionally, in-depth discussions of the software programs used in this analysis are not provided for the same rationale.

CONTENTS

Revision Log ii

Executive Summary iii

Contents v

Figures vii

Tables x

Acronymns xii

Introduction 1

Problem #1: 2D HZP BOC Pin Cell 3
Description and Specifications 3
Benchmark Results 4

Problem #2: 2D HZP BOC Fuel Lattice 5
Description and Specifications 5
Benchmark Results 7

Problem #3: 3D HZP Assembly 25
Design and Specifications 25
Benchmark Results 27

Problem #4: 3D HZP 3x3 Assembly Control Rod Worth 33
Description and Specifications 33
Benchmark Results 34

Problem #5: Physical Reactor Zero Power Physics Tests 37
Description and Specifications 37
Benchmark Results 39

Problem #6: 3D HFP Assembly 45
Description and Specifications 45
Benchmark Results 45

Problem #7: 3D HFP BOC Physical Reactor 48
Description and Benchmark 48
Benchmark Results 48

Problem #8: Physical Reactor Startup Flux Maps 53
Description and Specification 53
Benchmark Results 54

Problem #9: Physical Reactor Depletion 58
Description and Specification 58

Benchmark Results 61

Conclusions 65

References 66

FIGURES

Figure 1. Ten VERA Core Physics Benchmark Progression Problems (Ref. 2) 1

Figure P1-1. Problem 1 KENO-VI Geometry (Ref. 2) 3

Figure P2-1. Problem 2 Geometry (Ref. 2) 5

Figure P2-2. Problem 2 Lattice Layouts (Octant Symmetry) (Ref. 2) 6

Figure P2-3. Problem 2A Benchmark Results (Octant Symmetry), Showing KENO-VI, VERA and Percent Differences of Assembly Pin Powers (Ref. 2) 8

Figure P2-4. Problem 2B Benchmark Results (Octant Symmetry), Showing KENO-VI, VERA and Percent Differences of Assembly Pin Powers 9

Figure P2-5. Problem 2C Benchmark Results (Octant Symmetry), Showing KENO-VI, VERA and Percent Differences of Assembly Pin Powers 10

Figure P2-6. Problem 2D Benchmark Results (Octant Symmetry), Showing KENO-VI, VERA and Percent Differences of Assembly Pin Powers 11

Figure P2-7. Problem 2E Benchmark Results (Octant Symmetry), Showing KENO-VI, VERA and Percent Differences of Assembly Pin Powers 12

Figure P2-8. Problem 2F Benchmark Results (Octant Symmetry), Showing KENO-VI, VERA and Percent Differences of Assembly Pin Powers 13

Figure P2-9. Problem 2G Benchmark Results (Octant Symmetry), Showing KENO-VI, VERA and Percent Differences of Assembly Pin Powers 14

Figure P2-10. Problem 2H Benchmark Results (Octant Symmetry), Showing KENO-VI, VERA and Percent Differences of Assembly Pin Powers 15

Figure P2-11. Problem 2I Benchmark Results (Octant Symmetry), Showing KENO-VI, VERA and Percent Differences of Assembly Pin Powers 16

Figure P2-12. Problem 2J Benchmark Results (Octant Symmetry), Showing KENO-VI, VERA and Percent Differences of Assembly Pin Powers 17

Figure P2-13. Problem 2K Benchmark Results (Octant Symmetry), Showing KENO-VI, VERA and Percent Differences of Assembly Pin Powers 18

Figure P2-14. Problem 2L Benchmark Results (Octant Symmetry), Showing KENO-VI, VERA and Percent Differences of Assembly Pin Powers 19

Figure P2-15. Problem 2M Benchmark Results (Octant Symmetry), Showing KENO-VI, VERA and Percent Differences of Assembly Pin Powers 20

Figure P2-16. Problem 2N Benchmark Results (Octant Symmetry), Showing KENO-VI, VERA and Percent Differences of Assembly Pin Powers 21

Figure P2-17. Problem 2O Benchmark Results (Octant Symmetry), Showing KENO-VI, VERA and Percent Differences of Assembly Pin Powers 22

Figure P2-18. Problem 2P Benchmark Results (Octant Symmetry), Showing KENO-VI, VERA and Percent Differences of Assembly Pin Powers 23

Figure P2-19. Problem 2Q Benchmark Results (Octant Symmetry), Showing KENO-VI, VERA and Percent Differences of Assembly Pin Powers 24

Figure P3-1. Problem 3 Axial Geometry (without end plugs) [Left], Problem 3 Reference Model [Right] (Ref. 2).....26

Figure P3-2. Problem 3A Normalized Axial Power and Associated Difference for VERA Results (Ref. 2) 30

Figure P3-3. Problem 3A Normalized Axial Power and Associated Difference for VERA Results (Ref. 2) 30

Figure P3-4. Problem 3A Benchmark Results (Octant Symmetry), Showing KENO-VI, VERA and Percent Differences of Assembly Pin Powers 31

Figure P3-5. Problem 3B Benchmark Results (Octant Symmetry), Showing KENO-VI, VERA and Percent Differences of Assembly Pin Powers 32

Figure P4-1. Problem 4 Assembly, Poison, and Control Layout (Ref. 2) 33

Figure P4-1. Problem 4 Differential Rod Worths for KENO-VI and VERA (Ref. 2) 36

Figure P4-2. Problem 4 Integral Rod Worths for KENO-VI and VERA (Ref. 2).....36

Figure P5-1. Problem 5 Assembly, Poison, and Control Rod Layout, (Quarter Symmetry) (Ref. 2) 37

Figure P5-2. Problem 5 Benchmark Solution Criticals (Ref. 2).....40

Figure P5-3. Problem 5 Bank D Differential Worths for KENO-VI and VERA (Ref. 2).....41

Figure P5-4. Problem 5 Bank D Integral Rod Worths for KENO-VI and VERA (Ref. 2) 42

Figure P5-5. Problem 5 KENO-VI, VERA and Associated Differences for Radial Assembly Powers (Octant Symmetry).....43

Figure P5-5. Problem 5 [TOP] CE KENO-VI Radial Power Distribution and Uncertainty (%), [Bottom] VERA (Ref. 2).....44

Figure P6-1. Problem 6 Benchmark Results (Quadrant Symmetry), Showing MC21/CTF, VERA and Percent Differences of Pin Powers.....46

Figure P6-2. Problem 6 Visualization of Local Power Computed using VERA.....47

Figure P7-1. Problem 7 Benchmark Results (Quadrant Symmetry), Showing MC21/CTF, VERA and Percent Differences of Assembly Powers 49

Figure P7-2. Problem 7 Benchmark Results (Quadrant Symmetry), Showing MC21/CTF, VERA and Percent Differences of Core Exit Coolant Temperature in Kelvin 50

Figure P7-3. Problem 7 Visualization of Local Power Computed using VERA.....51

Figure P7-4. Axially-Averaged Pin Powers Computed using VERA and MC-21, (Quadrant Symmetry).....52

Figure P8-1. Card of Rod Removal Procedure and Reactor Power for Problem 8 (Ref. 2).....53

Figure P8-2. Critical Boron Concentration Plotted Against Reactor Power during the Specified Startup Procedure of Problem 8 (Ref. 2) 55

Figure P8-3. Assembly Averaged Power Peaking Factors for Problem 8 VERA Benchmark Results, Showing State Points 5, 29 and 49.....56

Figure P8-4. Axially Averaged Pin Power Peaking Factors for Problem 8 VERA Benchmark Results, Showing State Points 5, 29 and 49.....57

Figure P9-2. Problem 9 Model Input for Reactor Power (Ref. 2) 59

Figure P9-2. Problem 9 Measured and Computed Critical Boron Concentration (Ref. 2).....62

Figure P9-3. Axially-Averaged Pin Powers Computed using VERA for BOC, (Quadrant Symmetry) 62

Figure P9-4. Axially-Averaged Pin Powers Computed using VERA for MOC and EOC, (Quadrant Symmetry).....63

Figure P9-5. Axial Cross Section of the Simulated Reactor Showing Local Powers using VERA for BOC, MOC and EOC 64

TABLES

Table 1. Representative Runtimes of Benchmark Progression Problems, Indicating the Server and Problem Size 2

Table P1-1. Problem 1 Calculations (Ref. 2) 3

Table P1-2. Problem 1 Benchmark Results (Ref. 2) 4

Table P2-1. Problem 2 Calculations (Ref. 2) 5

Table P2-1. Problem 2 Benchmark Case Comparison (Ref. 2) 7

Table P3-1. Problem 3 Input Specification (Ref. 2) 25

Table P3-2. Problem 3 Reference Solution Results (Ref. 2) 27

Table P3-3. Problem 3 Axial Power Distribution for KENO and VERA, Bottom Portion (Ref. 2) 28

Table P3-4. Problem 3 Axial Power Distribution for KENO and VERA, Top Portion (Ref. 2) 29

Table P4-1. Problem 4 Specification (Ref. 2) 33

Table P4-2. Problem 4 Benchmark Problem Results Comparing VERA and KENO (Ref. 2) 34

Table P4-3. Problem 4 DRW and IRW for KENO-VI (Ref. 2) 35

Table P4-4. Problem 4 DRW and IRW for VERA 35

Table P5-1. Problem 5 Cases for WBN1 ZPPT (Ref. 2) 38

Table P5-2. Problem 5 Benchmark Results for WBN1 ZPPT (Ref. 2) 39

Table P5-7. Problem 5 Measured and Reference Solution ZPPT Results (Ref. 2) 41

Table P6-1. Problem 6 Specification (Ref. 2) 45

Table P6-2. Problem 6, Key Benchmark Results, Comparing Multiplication Factors and Pin Powers Differences (Ref. 6) 45

Table P7-1. Problem 7 Input Specification (Ref. 2) 48

Table P7-2. Problem 7, Key Benchmark Results, Comparing Critical Boron Concentration, Assembly Powers and Coolant Exit Temperatures (Ref. 6) 48

Table P8-1. Problem 8 Benchmark Case Results for VERA Computed Critical Boron Concentration for State Points 1-25 (Ref. 2) 54

Table P8-2. Problem 8 Benchmark Case Results for VERA Computed Critical Boron Concentration for State Points 26-49 (Ref. 2) 55

Table P9-1. Problem 9 Input Specification (Ref. 2) 58

Table P9-2. Problem 9 Approximate Shutdown Durations (Ref. 2).....59

Table P9-3. Problem 9 Cycle Depletion Specification (Ref. 2).....60

Table P9-4. Problem 9 Calculated Critical Boron Concentration for VERA Compared to Measured Data for State-points with Both Values (Ref. 2).....61

ACRONYMNS

2D	Two-Dimensional
3D	Three-Dimensional
AIC	Silver-Indium-Cadmium control rods
ARI	All Rods In
ARO	All Rods Out
B_4C	Boron Carbide control rods
BOC	Beginning-of-Cycle
BOL	Beginning-of-Life
CBW	Control Bank Reactivity Worth
CE	Continuous energy (as in cross sections)
CFD	Computational Fluid Dynamics
DBW	Differential Boron Reactivity Worth
DRW	Differential Control Rod Reactivity Worth
EFPD	Effective Full Power Day
EOC	End-of-Cycle
FP	Full Power
Gad	Gadolinia integral burnable absorber (Gd_2O_3)
GWd/MT	Gigawatt-day per metric ton (usually of Uranium)
HFP	Hot Full Power
HZP	Hot Zero Power
ITC	Isothermal Temperature Reactivity Coefficient
IFBA	Integral Fuel Burnable Absorber (here WEC's ZrB_2)
IRW	Integral Control Rod Reactivity Worth
LWR	Light Water Reactor
MG	Multi-group (as in cross sections)
NIST	National Institute of Standards and Technology
PCM	Percent milli (10^{-5})
PHI	Physics Integration Focus Area
PWR	Pressurized Water Reactor
RCCA	Rod Cluster Control Assembly
T/H	Thermal-Hydraulic
TVA	Tennessee Valley Authority
VERA	Virtual Environment for Reactor Applications
WABA	Wet Annular Burnable Absorber
WBN1	Watts Bar Nuclear Unit 1
WBN1C1	Watts Bar Nuclear Unit 1 Cycle 1
WEC	Westinghouse Electric Company
ZPPT	Zero Power Physics Tests

INTRODUCTION

The VERA Core Physics Benchmark Progression Problems (Figure 1) provide a method for developing and demonstrating increasing capabilities for reactor physics methods and software. They provide a model-based approach to prioritization of requirements, and create clear metrics to communicate development status. This document provides results to the first nine of these benchmark problems, ranging from a simple 2D pin cell to the full cycle depletion with control rods and burnable poisons consistent with actual nuclear power plant designs. Most of the specifications of benchmark problems are based on the initial core loading of Watts Bar Nuclear 1 (WBN1), a Westinghouse-designed 17x17 Pressurized Water Reactor (PWR). (Ref. 2)

Reference solutions to the benchmark problems are based on continuous energy (CE) Monte Carlo methods using ENDF/B-VII.0 (KENO-VI) or ENDF/B-VII.1 (MC21) cross sections. The successful calculation and subsequent agreement with reference solutions and measured data is designed to clearly demonstrate the capabilities of the VERA software.

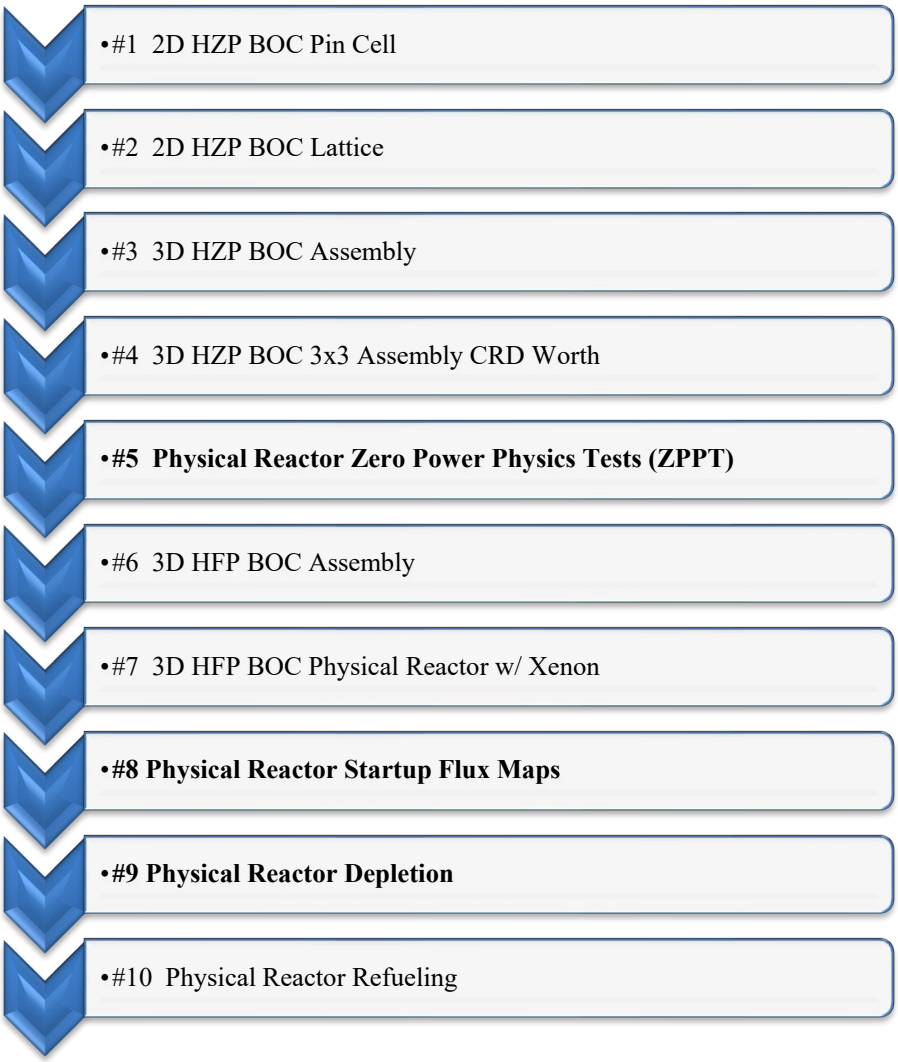

Figure 1. Ten VERA Core Physics Benchmark Progression Problems (Ref. 2)

This document contains brief descriptions of all ten problems, since more in-depth descriptions are provided in Godfrey (2014). It also contains results for benchmark problems 1 through 9. Problem 10 and other miscellaneous benchmarks will be added to this document in further revisions Reference solutions from a state-of-the-art program are included for each problem as are available and feasible to generate. These reference problems and available plant data are compared to the VERA results.

The VERA results were obtained using version 3.6, release candidate 0 (VERA 3.6-rc0). For the calculations performed, thermal expansion was not taken into account. This is because thermal expansion is not accounted for in KENO-VI. Problem calculations were performed on both Oak Ridge National Laboratory's EOS cluster and Idaho National Laboratory's FALCON cluster. Runtimes of representative problem can be seen compiled in Table 1. It can be seen that as the complexity of the problem increases, computation resources also increase. Problems 1 through 8 were able to be performed on less than 1000 cores, within 30 hours of runtime.

Table 1. Representative Runtimes of Benchmark Progression Problems, Indicating the Server and Problem Size

Problem	Size	Coupled CTF	Depletion State Points	Server	Cores	Runtime
1A	2D Pin Cell	No	N/A	FALCON	1	1.7 sec
2A	2D Assembly	No	N/A	FALCON	1	32 sec
3A	3D Assembly	No	N/A	FALCON	58	31 sec
4, Fully Withdrawn	3D 3x3 Assembly	No	N/A	FALCON	58	7.62 min
5, Case 1	3D Core	No	N/A	EOS	928	6.13 min
6	3D Assembly	Yes	N/A	FALCON	58	4.36 min
7	3D Core	Yes	N/A	EOS	928	30.58 min
8	3D Core	Yes	49	FALCON	928	28.5 h
9	3D Core	Yes	32	FALCON	928	29.5 h

PROBLEM #1: 2D HZP BOC PIN CELL

Description and Specifications

The first VERA core physics benchmark problem is a simple two-dimensional pin cell eigenvalue problem typical of PWR reactor analyses, as shown in Figure P1-1. It consists of a single Westinghouse 17x17-type fuel rod cell at beginning-of-life (BOL) conditions. The materials are standard for this type of reactor: UO_2, Zircaloy-4, and water. The moderator also contains soluble boron as a chemical shim for maintaining criticality. The pellet-clad gap consists of helium gas, but this material may be neglected due to its insignificant neutron cross section. (Ref. 2)

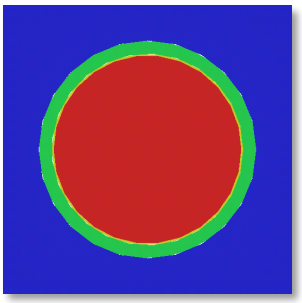

Figure P1-1. Problem 1 KENO-VI Geometry (Ref. 2)

This problem contains five separate calculations. The first (part A) represents typical zero power isothermal conditions which are representative of power reactor startup physics testing. Calculations B, C, and D are for the same rod geometry but with a range of fuel temperatures that are common under full power operating conditions. Problem 1E is an IFBA fuel rod. Problem specifications are contained in Table P1-1. (Ref. 1)

Table P1-1. Problem 1 Calculations (Ref. 2)

Problem	Moderator Temperature†	Fuel Temperature	Moderator Density
1A	565 K	565 K	0.743 g/cc
1B	600 K	600 K	0.661 g/cc
1C	↓	900 K	↓
1D	↓	1200 K	↓
1E	↓	600 K	0.743 g/cc

†Clad temperature set at moderator temperature

Benchmark Results

The results of the benchmark progression problem are contained in Table P1-2, showing the multiplication factor (K_{eff}). It can be seen that there is good agreement with KENO for all of the cases with the exception of the IFBA case, 1E. The difference between VERA and KENO is near 200 pcm for this case. This error is expected for MPACT when using the default ray spacing of 0.05 cm. If desired it could be reduced to improve the results, but this type of problem is not very realistic or indicative of an actual reactor problem. The differences for this cases can also be attributed to a small bias that exists due to the transport-corrected P0 scattering treatment employed. This bias is reduced and becomes insignificant when the problem size increases and becomes more realistic.

Table P1-2. Problem 1 Benchmark Results (Ref. 2)

Problem	Integral Absorber	Reference Solution – KENO-VI		VERA K_{eff}	Difference ($\Delta K \times 10^5$)
		K_{eff}	Uncertainty		
1A	None	1.18704	0.00005	1.18692	-127
1B	None	1.18215	0.00007	1.18208	-6
1C	None	1.17172	0.00007	1.17105	-67
1D	None	1.16260	0.00007	1.16176	-84
1E	IFBA	0.77169	0.00008	0.76975	-195

PROBLEM #2: 2D HZP BOC FUEL LATTICE

Description and Specifications

The second VERA core physics benchmark is a simple two-dimensional array of fuel rods (a fuel lattice) typical of the central axial region of PWR fuel assemblies. The problem consists of a single Westinghouse 17x17-type fuel lattice at beginning-of-life (BOL) as depicted in Figure P2-1. (Ref. 2)

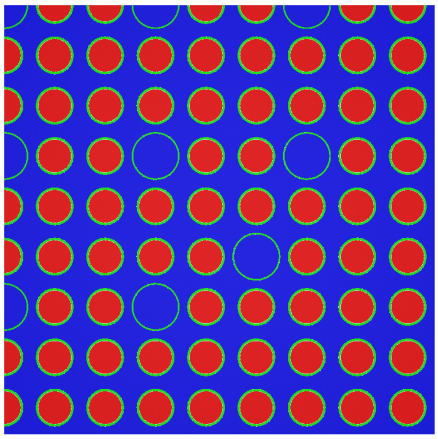

Figure P2-1. Problem 2 Geometry (Ref. 2)

In separate calculations based on this assembly, several materials such as silver-indium-cadmium (AIC), boron carbide (B_4C), Pyrex (B_2O_3-SiO_2), and B_4C-Al_2O_3 are used for neutron poisons inserted into the guide tubes. Integral burnable absorbers such as IFBA and Gadolinia are also included in some of the test cases. A full description of the case matrix can be seen in Table P2-1. (Ref. 2)

Table P2-1. Problem 2 Calculations (Ref. 2)

Problem	Description	Moderator and Cladding Temperature	Fuel Temperature	Moderator Density
2A	No Poisons	565 K	565 K	0.743 g/cc
2B	↓	600 K	600 K	0.661 g/cc
2C	↓	↓	900 K	↓
2D	↓	↓	1200 K	↓
2E	12 Pyrex	↓	600 K	0.743 g/cc
2F	24 Pyrex	↓	↓	↓
2G	24 AIC	↓	↓	↓
2H	24 B_4C	↓	↓	↓
2I	Instrument Thimble	↓	↓	↓
2J	Instrument + 24 Pyrex	↓	↓	↓
2K	Zoned + 24 Pyrex	↓	↓	↓
2L	80 IFBA	↓	↓	↓
2M	128 IFBA	↓	↓	↓
2N	104 IFBA + 20 WABA	↓	↓	↓
2O	12 Gadolinia	↓	↓	↓
2P	24 Gadolinia	↓	↓	↓
2Q	Zircaloy Spacer Grid	565 K	565 K	↓

Additionally, lattice layouts for each of the benchmark problems are provided in Figure P2-2 below. Locations of burnable poisons and water rods can clearly be seen.

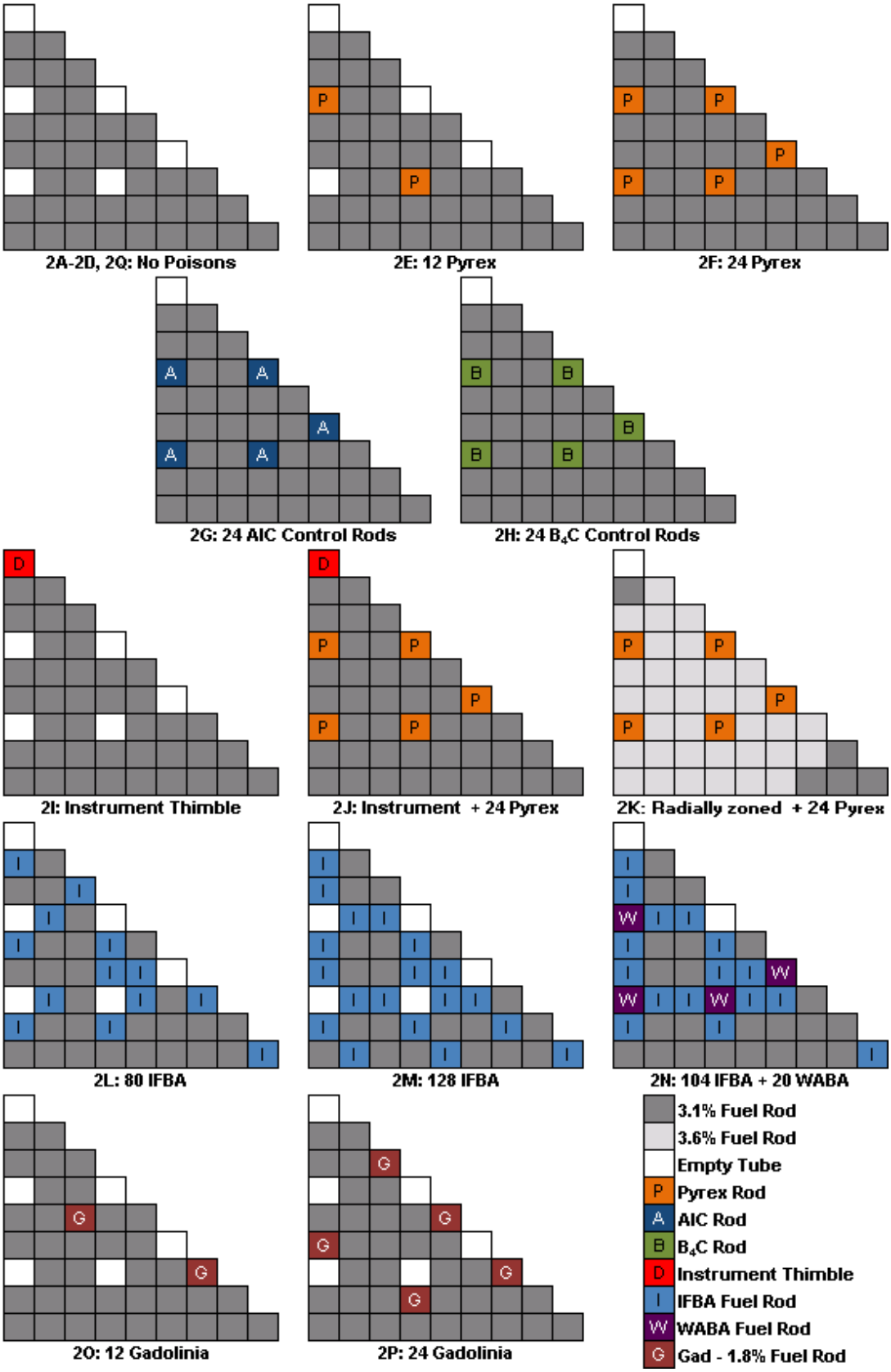

Figure P2-2. Problem 2 Lattice Layouts (Octant Symmetry) (Ref. 2)

Benchmark Results

TableP2-1 contains the results from the CE KENO-VI reference calculations and the VERA calculations. Displayed in the table are multiplication factor (K_{eff}), associated differences, the maximum power difference between the benchmark (in percent) and VERA and the root mean squares (RMS) difference in pin power (in percent).

Table P2-1. Problem 2 Benchmark Case Comparison (Ref. 2)

Problem	Description	KENO-VI K_{eff}	VERA K_{eff}	Difference ($\Delta K x 10^5$)	ΔP RMS (%)	ΔP MAX (%)
2A	No Poisons	1.18218	1.18213	-5	0.11	0.23
2B	No Poisons	1.18336	1.18337	1	0.08	0.20
2C	No Poisons	1.17375	1.17333	-42	0.09	0.19
2D	No Poisons	1.16559	1.16485	-74	0.07	0.17
2E	12 Pyrex	1.06963	1.07042	79	0.07	0.19
2F	24 Pyrex	0.97602	0.97735	134	0.11	0.23
2G	24 AIC	0.84770	0.85178	409	0.23	0.54
2H	24 B_4C	0.78822	0.79260	438	0.25	0.59
2I	Instrument Thimble	1.17992	1.17988	-3	0.08	0.19
2J	Instrument + 24 Pyrex	0.97519	0.97660	141	0.10	0.21
2K	Zoned + 24 Pyrex	1.02006	1.02147	140	0.11	0.24
2L	80 IFBA	1.01892	1.01914	23	0.08	0.19
2M	128 IFBA	0.93880	0.93937	57	0.09	0.23
2N	104 IFBA + 20 WABA	0.86962	0.86993	31	0.07	0.15
2O	12 Gadolinia	1.04773	1.04750	-23	0.13	0.30
2P	24 Gadolinia	0.92741	0.92687	-54	0.19	0.54
2Q	Zircaloy Spacer Grid	1.17194	1.17168	-26	0.09	0.20

It can be seen that as the amount of AIC, B_4C or Pyrex increases, the agreement between VERA and KENO diverges. VERA consistently shows a higher multiplication factor in these cases with the difference being largest for the AIC and B_4C cases. These cases have the lowest overall multiplication factors. The differences for these cases can be attributed to a small bias that exists due to the transport-corrected P0 scattering treatment employed. This bias is reduced and becomes insignificant when the problem size increases and becomes more realistic. This is additionally the reason for case 1E having a large difference in multiplication factor.

The subsequent figures display the calculated normalized fission rate distributions (pin powers) for both the KENO and VERA calculations for cases 2A-2Q. Associated reaction rate uncertainties can be seen in Godfrey (2014). It is to be noted that the reference KENO-VI results are calculated in quarter assembly geometry, but are collapsed to one eighth assembly results; symmetric fuel rod powers are averaged.

1.0364	1.0089							
1.0371	1.0093	1.0104						
	1.0368	1.0386						
1.0353	1.0089	1.0118	1.0451	1.0313				
1.0328	1.0053	1.0089	1.0458	1.0516				
	1.0266	1.0281		1.0360	1.0180	0.9736		
1.0122	0.9880	0.9880	1.0115	0.9837	0.9649	0.9483	0.9389	
0.9764	0.9721	0.9714	0.9739	0.9645	0.9551	0.9458	0.9418	0.9476

KENO-VI

1.0350	1.0097							
1.0359	1.0106	1.0104						
	1.0364	1.0370						
1.0342	1.0086	1.0113	1.0437	1.0335				
1.0311	1.0061	1.0097	1.0435	1.0514				
	1.0247	1.0267		1.0362	1.0171	0.9740		
1.0106	0.9888	0.9892	1.0113	0.9835	0.9641	0.9491	0.9403	
0.9762	0.9725	0.9725	0.9743	0.9657	0.9559	0.9470	0.9432	0.9487

VERA

-0.14	0.08							
-0.12	0.13	0.00						
	-0.04	-0.16						
-0.11	-0.03	-0.05	-0.14	0.22				
-0.17	0.08	0.08	-0.23	-0.02				
	-0.19	-0.14		0.02	-0.09	0.04		
-0.16	0.08	0.12	-0.02	-0.02	-0.08	0.08	0.14	
-0.02	0.04	0.11	0.04	0.12	0.08	0.12	0.14	0.11

Difference (%)

Figure P2-3. Problem 2A Benchmark Results (Octant Symmetry), Showing KENO-VI, VERA and Percent Differences of Assembly Pin Powers (Ref. 2)

1.0355	1.0113							
1.0362	1.0113	1.0121						
	1.0359	1.0373						
1.0337	1.0099	1.0124	1.0424	1.0308				
1.0308	1.0066	1.0095	1.0427	1.0474				
	1.0243	1.0258		1.0326	1.0146	0.9745		
1.0103	0.9893	0.9893	1.0099	0.9839	0.9666	0.9503	0.9406	
0.9781	0.9742	0.9738	0.9752	0.9662	0.9565	0.9475	0.9435	0.9478

KENO-VI (Ref. 2)

1.0345	1.0116							
1.0353	1.0124	1.0120						
	1.0355	1.0360						
1.0331	1.0098	1.0123	1.0415	1.0323				
1.0298	1.0071	1.0103	1.0407	1.0477				
	1.0231	1.0249		1.0330	1.0146	0.9744		
1.0098	0.9899	0.9901	1.0099	0.9839	0.9651	0.9507	0.9419	
0.9778	0.9745	0.9742	0.9754	0.9670	0.9572	0.9483	0.9442	0.9489

VERA

-0.10	0.03							
-0.09	0.11	-0.01						
	-0.04	-0.13						
-0.06	-0.01	-0.01	-0.09	0.15				
-0.10	0.05	0.08	-0.20	0.03				
	-0.12	-0.09		0.04	0.00	-0.01		
-0.05	0.06	0.08	0.00	0.00	-0.15	0.04	0.13	
-0.03	0.03	0.04	0.02	0.08	0.07	0.08	0.07	0.11

Difference (%)

Figure P2-4. Problem 2B Benchmark Results (Octant Symmetry), Showing KENO-VI, VERA and Percent Differences of Assembly Pin Powers

1.0357	1.0109							
1.0364	1.0113	1.0124						
	1.0364	1.0375						
1.0346	1.0102	1.0124	1.0422	1.0306				
1.0306	1.0066	1.0095	1.0426	1.0473				
	1.0248	1.0259		1.0324	1.0150	0.9738		
1.0102	0.9891	0.9891	1.0102	0.9840	0.9666	0.9494	0.9411	
0.9782	0.9742	0.9738	0.9753	0.9658	0.9564	0.9476	0.9433	0.9476

KENO-VI (Ref. 2)

1.0347	1.0117							
1.0355	1.0124	1.0121						
	1.0356	1.0361						
1.0332	1.0099	1.0123	1.0416	1.0323				
1.0298	1.0071	1.0103	1.0407	1.0478				
	1.0232	1.0250		1.0330	1.0146	0.9743		
1.0098	0.9899	0.9900	1.0099	0.9839	0.9650	0.9505	0.9418	
0.9778	0.9744	0.9742	0.9754	0.9669	0.9571	0.9481	0.9440	0.9488

VERA

-0.10	0.08							
-0.09	0.11	-0.03						
	-0.08	-0.14						
-0.14	-0.03	-0.01	-0.06	0.17				
-0.08	0.05	0.08	-0.19	0.05				
	-0.16	-0.09		0.06	-0.04	0.05		
-0.04	0.08	0.09	-0.03	-0.01	-0.16	0.11	0.07	
-0.04	0.02	0.04	0.01	0.11	0.07	0.05	0.07	0.12

Difference (%)

Figure P2-5. Problem 2C Benchmark Results (Octant Symmetry), Showing KENO-VI, VERA and Percent Differences of Assembly Pin Powers

1.0360	1.0115							
1.0364	1.0119	1.0122						
	1.0364	1.0379						
1.0342	1.0100	1.0122	1.0426	1.0313				
1.0305	1.0067	1.0097	1.0419	1.0474				
	1.0243	1.0258		1.0327	1.0148	0.9741		
1.0111	0.9895	0.9891	1.0100	0.9836	0.9657	0.9499	0.9404	
0.9785	0.9741	0.9737	0.9752	0.9664	0.9565	0.9474	0.9426	0.9477

KENO-VI (Ref. 2)

1.0348	1.0117							
1.0356	1.0125	1.0121						
	1.0357	1.0362						
1.0333	1.0099	1.0124	1.0417	1.0324				
1.0299	1.0071	1.0103	1.0408	1.0479				
	1.0233	1.0251		1.0331	1.0146	0.9742		
1.0099	0.9899	0.9900	1.0099	0.9838	0.9649	0.9504	0.9416	
0.9777	0.9744	0.9741	0.9753	0.9668	0.9570	0.9480	0.9439	0.9486

VERA

-0.12	0.02							
-0.08	0.06	-0.01						
	-0.07	-0.17						
-0.09	-0.01	0.02	-0.09	0.11				
-0.06	0.04	0.06	-0.11	0.05				
	-0.10	-0.07		0.04	-0.02	0.01		
-0.12	0.04	0.09	-0.01	0.02	-0.08	0.05	0.12	
-0.08	0.03	0.04	0.01	0.04	0.05	0.06	0.13	0.09

Difference (%)

Figure P2-6. Problem 2D Benchmark Results (Octant Symmetry), Showing KENO-VI, VERA and Percent Differences of Assembly Pin Powers

1.0170	0.9930							
0.9299	0.9635	0.9962						
	0.9331	1.0250						
0.9347	0.9695	1.0022	1.0362	1.0290				
1.0290	1.0034	0.9751	0.9523	1.0226				
	1.0350	0.9419		0.9579	1.0426	1.0314		
1.0578	1.0222	0.9763	0.9355	0.9787	1.0146	1.0246	1.0290	
1.0346	1.0238	1.0054	0.9938	1.0054	1.0218	1.0314	1.0398	1.0514

KENO-VI (Ref. 2)

1.0178	0.9930							
0.9307	0.9636	0.9959						
	0.9337	1.0248						
0.9352	0.9676	1.0025	1.0368	1.0303				
1.0289	1.0033	0.9747	0.9519	1.0226				
	1.0347	0.9426		0.9591	1.0431	1.0319		
1.0573	1.0221	0.9763	0.9364	0.9777	1.0128	1.0244	1.0299	
1.0335	1.0228	1.0057	0.9948	1.0055	1.0212	1.0316	1.0399	1.0517

VERA

0.08	0.00							
0.08	0.01	-0.03						
	0.06	-0.02						
0.05	-0.19	0.03	0.06	0.13				
-0.01	-0.01	-0.04	-0.04	0.00				
	-0.03	0.07		0.12	0.05	0.05		
-0.05	-0.01	0.00	0.09	-0.10	-0.18	-0.02	0.09	
-0.11	-0.10	0.03	0.10	0.01	-0.06	0.02	0.01	0.03

Difference (%)

Figure P2-7. Problem 2E Benchmark Results (Octant Symmetry), Showing KENO-VI, VERA and Percent Differences of Assembly Pin Powers

1.0783	1.0428							
0.9714	0.9907	0.9736						
	0.9333	0.9262						
0.9258	0.9591	0.9543	0.9118	0.9262				
0.9280	0.9617	0.9587	0.9127	0.9070				
	0.9420	0.9411		0.9350	0.9670	1.0340		
0.9744	1.0047	1.0060	0.9793	1.0191	1.0502	1.0831	1.1094	
1.0472	1.0529	1.0551	1.0551	1.0717	1.0923	1.1138	1.1339	1.1541

KENO-VI (Ref. 2)

1.0769	1.0423							
0.9717	0.9902	0.9715						
	0.9347	0.9275						
0.9273	0.9577	0.9540	0.9134	0.9266				
0.9298	0.9612	0.9582	0.9150	0.9078				
	0.9429	0.9426		0.9357	0.9685	1.0327		
0.9742	1.0037	1.0051	0.9796	1.0176	1.0495	1.0819	1.1094	
1.0473	1.0523	1.0550	1.0561	1.0718	1.0914	1.1128	1.1328	1.1526

VERA

-0.14	-0.05							
0.03	-0.05	-0.21						
	0.14	0.13						
0.15	-0.14	-0.03	0.16	0.04				
0.18	-0.05	-0.05	0.23	0.08				
	0.09	0.15		0.07	0.15	-0.13		
-0.02	-0.10	-0.09	0.03	-0.15	-0.07	-0.12	0.00	
0.01	-0.06	-0.01	0.10	0.01	-0.09	-0.10	-0.11	-0.15

Difference (%)

Figure P2-8. Problem 2F Benchmark Results (Octant Symmetry), Showing KENO-VI, VERA and Percent Differences of Assembly Pin Powers

1.0732	1.0353							
0.9393	0.9660	0.9411						
	0.8855	0.8762						
0.8736	0.9200	0.9138	0.8529	0.8719				
0.8784	0.9273	0.9212	0.8559	0.8507				
	0.9083	0.9072		0.9070	0.9646	1.0707		
0.9646	1.0058	1.0098	0.9778	1.0394	1.0944	1.1525	1.1999	
1.0707	1.0803	1.0858	1.0899	1.1202	1.1585	1.2005	1.2363	1.2666

KENO-VI (Ref. 2)

1.0744	1.0348							
0.9404	0.9648	0.9389						
	0.8889	0.8779						
0.8764	0.9189	0.9130	0.8568	0.8721				
0.8821	0.9260	0.9212	0.8613	0.8534				
	0.9096	0.9102		0.9081	0.9678	1.0699		
0.9644	1.0044	1.0083	0.9781	1.0368	1.0933	1.1500	1.1975	
1.0710	1.0785	1.0843	1.0906	1.1194	1.1571	1.1972	1.2324	1.2617

VERA

0.12	-0.05							
0.11	-0.12	-0.22						
	0.34	0.17						
0.28	-0.11	-0.08	0.39	0.02				
0.37	-0.13	0.00	0.54	0.27				
	0.13	0.30		0.11	0.32	-0.08		
-0.02	-0.14	-0.15	0.03	-0.26	-0.11	-0.25	-0.24	
0.03	-0.18	-0.15	0.07	-0.08	-0.14	-0.33	-0.39	-0.49

Difference (%)

Figure P2-9. Problem 2G Benchmark Results (Octant Symmetry), Showing KENO-VI, VERA and Percent Differences of Assembly Pin Powers

1.0607	1.0215							
0.9221	0.9481	0.9210						
	0.8646	0.8547						
0.8516	0.9001	0.8931	0.8311	0.8511				
0.8589	0.9093	0.9032	0.8361	0.8344				
	0.8952	0.8962		0.9022	0.9707	1.0905		
0.9609	1.0041	1.0104	0.9802	1.0495	1.1144	1.1840	1.2416	
1.0751	1.0862	1.0943	1.1019	1.1405	1.1873	1.2384	1.2829	1.3188

KENO-VI (Ref. 2)

1.0625	1.0217							
0.9231	0.9475	0.9201						
	0.8684	0.8581						
0.8551	0.8987	0.8928	0.8347	0.8500				
0.8636	0.9090	0.9039	0.8417	0.8345				
	0.8990	0.8991		0.9021	0.9721	1.0882		
0.9618	1.0032	1.0085	0.9803	1.0464	1.1132	1.1807	1.2378	
1.0771	1.0850	1.0927	1.1032	1.1386	1.1856	1.2352	1.2786	1.3129

VERA

0.18	0.02							
0.10	-0.06	-0.09						
	0.38	0.34						
0.35	-0.14	-0.03	0.36	-0.11				
0.47	-0.03	0.07	0.56	0.01				
	0.38	0.29		-0.01	0.14	-0.23		
0.09	-0.09	-0.19	0.01	-0.31	-0.12	-0.33	-0.38	
0.20	-0.12	-0.16	0.13	-0.19	-0.17	-0.32	-0.43	-0.59

Difference (%)

Figure P2-10. Problem 2H Benchmark Results (Octant Symmetry), Showing KENO-VI, VERA and Percent Differences of Assembly Pin Powers

1.0045	0.9929							
1.0251	1.0023	1.0073						
	1.0334	1.0367						
1.0352	1.0088	1.0117	1.0450	1.0327				
1.0327	1.0070	1.0102	1.0457	1.0515				
	1.0269	1.0287		1.0370	1.0189	0.9755		
1.0128	0.9900	0.9903	1.0128	0.9856	0.9679	0.9513	0.9415	
0.9791	0.9748	0.9748	0.9759	0.9679	0.9574	0.9487	0.9444	0.9502

KENO-VI (Ref. 2)

1.0038	0.9927							
1.0254	1.0036	1.0069						
	1.0334	1.0354						
1.0333	1.0086	1.0118	1.0439	1.0345				
1.0315	1.0072	1.0110	1.0442	1.0520				
	1.0257	1.0278		1.0371	1.0184	0.9761		
1.0120	0.9908	0.9911	1.0127	0.9856	0.9664	0.9516	0.9428	
0.9785	0.9748	0.9748	0.9766	0.9680	0.9583	0.9494	0.9456	0.9509

VERA

-0.07	-0.02							
0.03	0.13	-0.04						
	0.00	-0.13						
-0.19	-0.02	0.01	-0.11	0.18				
-0.12	0.02	0.08	-0.15	0.05				
	-0.12	-0.09		0.01	-0.05	0.06		
-0.08	0.08	0.08	-0.01	0.00	-0.15	0.03	0.13	
-0.06	0.00	0.00	0.07	0.01	0.09	0.07	0.12	0.07

Difference (%)

Figure P2-11. Problem 2I Benchmark Results (Octant Symmetry), Showing KENO-VI, VERA and Percent Differences of Assembly Pin Powers

1.0415	1.0226							
0.9590	0.9823	0.9683						
	0.9305	0.9248						
0.9262	0.9590	0.9555	0.9130	0.9288				
0.9288	0.9630	0.9595	0.9143	0.9086				
	0.9428	0.9428		0.9371	0.9696	1.0358		
0.9762	1.0060	1.0077	0.9805	1.0213	1.0529	1.0849	1.1121	
1.0489	1.0555	1.0577	1.0577	1.0744	1.0941	1.1160	1.1362	1.1559

KENO-VI (Ref. 2)

1.0406	1.0218							
0.9601	0.9817	0.9672						
	0.9320	0.9262						
0.9271	0.9576	0.9544	0.9143	0.9279				
0.9308	0.9623	0.9594	0.9164	0.9095				
	0.9444	0.9442		0.9376	0.9706	1.0349		
0.9761	1.0056	1.0070	0.9815	1.0197	1.0517	1.0843	1.1119	
1.0494	1.0544	1.0571	1.0583	1.0740	1.0938	1.1152	1.1353	1.1551

VERA

-0.09	-0.08							
0.11	-0.06	-0.11						
	0.15	0.14						
0.09	-0.14	-0.11	0.13	-0.09				
0.20	-0.07	-0.01	0.21	0.09				
	0.16	0.14		0.05	0.10	-0.09		
-0.01	-0.04	-0.07	0.10	-0.16	-0.12	-0.06	-0.02	
0.05	-0.11	-0.06	0.06	-0.04	-0.03	-0.08	-0.09	-0.08

Difference (%)

Figure P2-12. Problem 2J Benchmark Results (Octant Symmetry), Showing KENO-VI, VERA and Percent Differences of Assembly Pin Powers

0.9765	1.0637							
0.9899	1.0055	0.9849						
	0.9455	0.9388						
0.9380	0.9690	0.9644	0.9237	0.9388				
0.9388	0.9707	0.9673	0.9246	0.9195				
	0.9510	0.9505		0.9476	0.9807	1.0495		
0.9811	1.0105	1.0122	0.9874	1.0285	1.0645	1.1073	1.0159	
1.0524	1.0578	1.0608	1.0620	1.0813	1.1098	1.0147	1.0453	1.0687

KENO-VI (Ref. 2)

0.9762	1.0632							
0.9897	1.0044	0.9834						
	0.9475	0.9398						
0.9388	0.9677	0.9641	0.9255	0.9381				
0.9406	0.9703	0.9677	0.9270	0.9205				
	0.9523	0.9523		0.9478	0.9821	1.0490		
0.9815	1.0098	1.0115	0.9883	1.0270	1.0633	1.1064	1.0146	
1.0523	1.0570	1.0601	1.0628	1.0810	1.1092	1.0139	1.0437	1.0673

VERA

-0.03	-0.05							
-0.02	-0.11	-0.15						
	0.20	0.10						
0.08	-0.13	-0.03	0.18	-0.07				
0.18	-0.04	0.04	0.24	0.10				
	0.13	0.18		0.02	0.14	-0.05		
0.04	-0.07	-0.07	0.09	-0.15	-0.12	-0.09	-0.13	
-0.01	-0.08	-0.07	0.08	-0.03	-0.06	-0.08	-0.16	-0.14

Difference (%)

Figure P2-13. Problem 2K Benchmark Results (Octant Symmetry), Showing KENO-VI, VERA and Percent Differences of Assembly Pin Powers

0.9481	0.9967							
1.0328	1.0001	0.9313						
	0.9556	1.0286						
0.9606	1.0093	1.0106	0.9409	0.9816				
1.0475	1.0219	1.0160	0.9405	0.9388				
	0.9690	1.0466		0.9544	1.0332	0.9388		
0.9644	1.0198	1.0273	0.9648	1.0152	1.0223	1.0093	1.0076	
1.0311	1.0362	1.0383	1.0307	1.0341	1.0353	1.0257	1.0026	0.9053

KENO-VI (Ref. 2)

0.9484	0.9983							
1.0322	1.0010	0.9306						
	0.9544	1.0280						
0.9593	1.0106	1.0112	0.9400	0.9835				
1.0467	1.0227	1.0162	0.9389	0.9390				
	0.9678	1.0458		0.9539	1.0328	0.9394		
0.9640	1.0206	1.0278	0.9643	1.0160	1.0221	1.0100	1.0084	
1.0307	1.0361	1.0372	1.0302	1.0339	1.0355	1.0266	1.0032	0.9067

VERA

0.03	0.16							
-0.06	0.09	-0.07						
	-0.12	-0.06						
-0.13	0.13	0.06	-0.09	0.19				
-0.08	0.08	0.02	-0.16	0.02				
	-0.12	-0.08		-0.05	-0.04	0.06		
-0.04	0.08	0.05	-0.05	0.08	-0.02	0.07	0.08	
-0.04	-0.01	-0.11	-0.05	-0.02	0.02	0.09	0.06	0.14

Difference (%)

Figure P2-14. Problem 2L Benchmark Results (Octant Symmetry), Showing KENO-VI, VERA and Percent Differences of Assembly Pin Powers

0.9833	1.0389							
0.9846	1.0393	1.0389						
	0.9833	0.9824						
0.9828	1.0370	1.0361	0.9760	1.0206				
0.9814	1.0361	1.0343	0.9714	0.9696				
	0.9769	0.9778		0.9696	0.9659	1.0042		
0.9728	1.0193	1.0297	0.9792	1.0170	1.0170	0.9441	1.0152	
1.0079	0.9432	1.0334	1.0288	0.9473	1.0325	1.0361	1.0306	0.9423

KENO-VI (Ref. 2)

0.9826	1.0398							
0.9823	1.0394	1.0393						
	0.9820	0.9812						
0.9819	1.0384	1.0366	0.9751	1.0226				
0.9805	1.0368	1.0350	0.9698	0.9695				
	0.9764	0.9770		0.9697	0.9653	1.0054		
0.9721	1.0203	1.0308	0.9779	1.0185	1.0161	0.9441	1.0162	
1.0079	0.9433	1.0330	1.0289	0.9470	1.0323	1.0374	1.0309	0.9434

VERA

-0.07	0.09							
-0.23	0.01	0.04						
	-0.13	-0.12						
-0.09	0.14	0.05	-0.09	0.20				
-0.09	0.07	0.07	-0.16	-0.01				
	-0.05	-0.08		0.01	-0.06	0.12		
-0.07	0.10	0.11	-0.13	0.15	-0.09	0.00	0.10	
0.00	0.01	-0.04	0.01	-0.03	-0.02	0.13	0.03	0.11

Difference (%)

Figure P2-15. Problem 2M Benchmark Results (Octant Symmetry), Showing KENO-VI, VERA and Percent Differences of Assembly Pin Powers

0.9756	1.0258							
0.8993	0.9963	1.0209						
	0.8923	0.9657						
0.8697	0.9722	1.0057	0.9468	0.9557				
0.8678	0.9644	0.9700	0.8651	0.8467				
	0.8819	0.8831		0.8705	0.9111	1.0554		
0.9247	1.0155	1.0180	0.9318	1.0367	1.0824	1.1272	1.1538	
1.0800	1.0928	1.0962	1.0923	1.1184	1.1459	1.1661	1.1602	1.0603

KENO-VI (Ref. 2)

0.9751	1.0261							
0.8982	0.9949	1.0215						
	0.8912	0.9649						
0.8699	0.9714	1.0058	0.9465	0.9563				
0.8682	0.9637	0.9695	0.8653	0.8466				
	0.8826	0.8836		0.8706	0.9119	1.0556		
0.9250	1.0153	1.0174	0.9315	1.0360	1.0833	1.1281	1.1541	
1.0815	1.0923	1.0955	1.0929	1.1185	1.1466	1.1670	1.1610	1.0608

VERA

-0.05	0.03							
-0.11	-0.14	0.06						
	-0.11	-0.08						
0.02	-0.08	0.01	-0.03	0.06				
0.04	-0.07	-0.05	0.02	-0.01				
	0.07	0.05		0.01	0.08	0.02		
0.03	-0.02	-0.06	-0.03	-0.07	0.09	0.09	0.03	
0.15	-0.05	-0.07	0.06	0.01	0.07	0.09	0.08	0.05

Difference (%)

Figure P2-16. Problem 2N Benchmark Results (Octant Symmetry), Showing KENO-VI, VERA and Percent Differences of Assembly Pin Powers

1.1049	1.0710							
1.0889	1.0505	1.0180						
	1.0408	0.9805						
1.0478	0.9658	0.2175	0.9882	1.0367				
1.0726	1.0225	0.9772	1.0555	1.0812				
	1.0926	1.0824		1.0788	0.9931	0.2173		
1.1053	1.0779	1.0722	1.0918	1.0478	0.9931	0.9254	0.9641	
1.0771	1.0714	1.0677	1.0637	1.0429	1.0168	0.9935	0.9996	1.0164

KENO-VI (Ref. 2)

1.1031	1.0704							
1.0874	1.0508	1.0194						
	1.0391	0.9796						
1.0478	0.9669	0.2145	0.9880	1.0396				
1.0716	1.0222	0.9793	1.0529	1.0816				
	1.0910	1.0824		1.0800	0.9939	0.2145		
1.1036	1.0784	1.0737	1.0919	1.0478	0.9910	0.9271	0.9645	
1.0768	1.0716	1.0680	1.0640	1.0435	1.0170	0.9948	1.0008	1.0176

VERA

-0.18	-0.06							
-0.15	0.03	0.14						
	-0.17	-0.09						
0.00	0.11	-0.30	-0.02	0.29				
-0.10	-0.03	0.21	-0.26	0.04				
	-0.16	0.00		0.12	0.08	-0.28		
-0.17	0.05	0.15	0.01	0.00	-0.21	0.17	0.04	
-0.03	0.02	0.03	0.03	0.06	0.02	0.13	0.12	0.12

Difference (%)

Figure P2-17. Problem 2O Benchmark Results (Octant Symmetry), Showing KENO-VI, VERA and Percent Differences of Assembly Pin Powers

1.1688	1.1160							
1.1411	1.0530	0.2442						
	1.1180	1.0636						
1.0659	1.0821	1.0881	1.0627	0.2443				
0.2459	1.0401	1.0950	1.1088	1.0608				
	1.1148	1.1070		1.0807	1.0378	0.2431		
1.1476	1.1088	1.0332	0.2440	1.0078	1.0406	1.0050	1.0608	
1.1337	1.1143	1.0641	0.9954	1.0438	1.0751	1.0821	1.1051	1.1300

KENO-VI (Ref. 2)

1.1662	1.1106							
1.1419	1.0549	0.2409						
	1.1156	1.0629						
1.0663	1.0817	1.0890	1.0621	0.2411				
0.2424	1.0418	1.0968	1.1057	1.0611				
	1.1130	1.1055		1.0828	1.0384	0.2400		
1.1468	1.1102	1.0356	0.2409	1.0090	1.0397	1.0074	1.0618	
1.1322	1.1139	1.0631	0.9977	1.0438	1.0758	1.0842	1.1063	1.1314

VERA

-0.26	-0.54							
0.08	0.19	-0.33						
	-0.24	-0.07						
0.04	-0.04	0.09	-0.06	-0.32				
-0.35	0.17	0.18	-0.31	0.03				
	-0.18	-0.15		0.21	0.06	-0.31		
-0.08	0.14	0.24	-0.31	0.12	-0.09	0.24	0.10	
-0.15	-0.04	-0.10	0.23	0.00	0.07	0.21	0.12	0.14

Difference (%)

Figure P2-18. Problem 2P Benchmark Results (Octant Symmetry), Showing KENO-VI, VERA and Percent Differences of Assembly Pin Powers

1.0368	1.0105							
1.0371	1.0113	1.0120						
	1.0375	1.0389						
1.0353	1.0098	1.0124	1.0448	1.0331				
1.0320	1.0069	1.0098	1.0448	1.0513				
	1.0258	1.0273		1.0357	1.0160	0.9726		
1.0113	0.9883	0.9879	1.0109	0.9828	0.9639	0.9468	0.9369	
0.9774	0.9726	0.9723	0.9745	0.9646	0.9548	0.9457	0.9413	0.9479

KENO-VI (Ref. 2)

1.0356	1.0110							
1.0364	1.0118	1.0118						
	1.0369	1.0376						
1.0342	1.0093	1.0124	1.0438	1.0343				
1.0308	1.0065	1.0104	1.0431	1.0512				
	1.0243	1.0263		1.0355	1.0156	0.9728		
1.0102	0.9889	0.9894	1.0108	0.9832	0.9630	0.9478	0.9389	
0.9765	0.9733	0.9732	0.9745	0.9657	0.9554	0.9462	0.9423	0.9484

VERA

-0.12	0.05							
-0.07	0.05	-0.02						
	-0.06	-0.13						
-0.11	-0.05	0.00	-0.10	0.12				
-0.12	-0.04	0.06	-0.17	-0.01				
	-0.15	-0.10		-0.02	-0.04	0.02		
-0.11	0.06	0.15	-0.01	0.04	-0.09	0.10	0.20	
-0.09	0.07	0.09	0.00	0.11	0.06	0.05	0.10	0.05

Difference (%)

Figure P2-19. Problem 2Q Benchmark Results (Octant Symmetry), Showing KENO-VI, VERA and Percent Differences of Assembly Pin Powers

PROBLEM #3: 3D HZP ASSEMBLY

Design and Specifications

This benchmark problems is two separate cases of a three dimensional assembly at hot zero power. The cases are a typical Westinghouse 17x17-type fuel assembly at beginning-of-life (BOL) and Hot Zero Power (HZP) isothermal conditions, based on WBN1. The moderator contains soluble boron as a chemical shim for maintaining criticality. This problem has two separate cases, the first has a slightly higher enrichment and no poisons, while the second has a lower enrichment and 16 Pyrex rods. The differences in these calculations are described in Table P3-1 below. (Ref. 2)

Table P3-1. Problem 3 Input Specification (Ref. 2)

Input	3A	3B
Fuel Density	10.257 g/cc	10.257 g/cc
Fuel Enrichment	3.1%	2.619%
Power	0% FP	0% FP
Inlet Coolant Temperature	600 K	565 K
Inlet Coolant Density	0.743 g/cc	0.743 g/cc
Reactor Pressure	2250 psia	2250 psia
Boron Concentration	1300 ppm	1066 ppm
Pyrex Burnable Poison Pattern	None	16

The axial geometry of the problem and a reference model can be found in Figure P3-1.

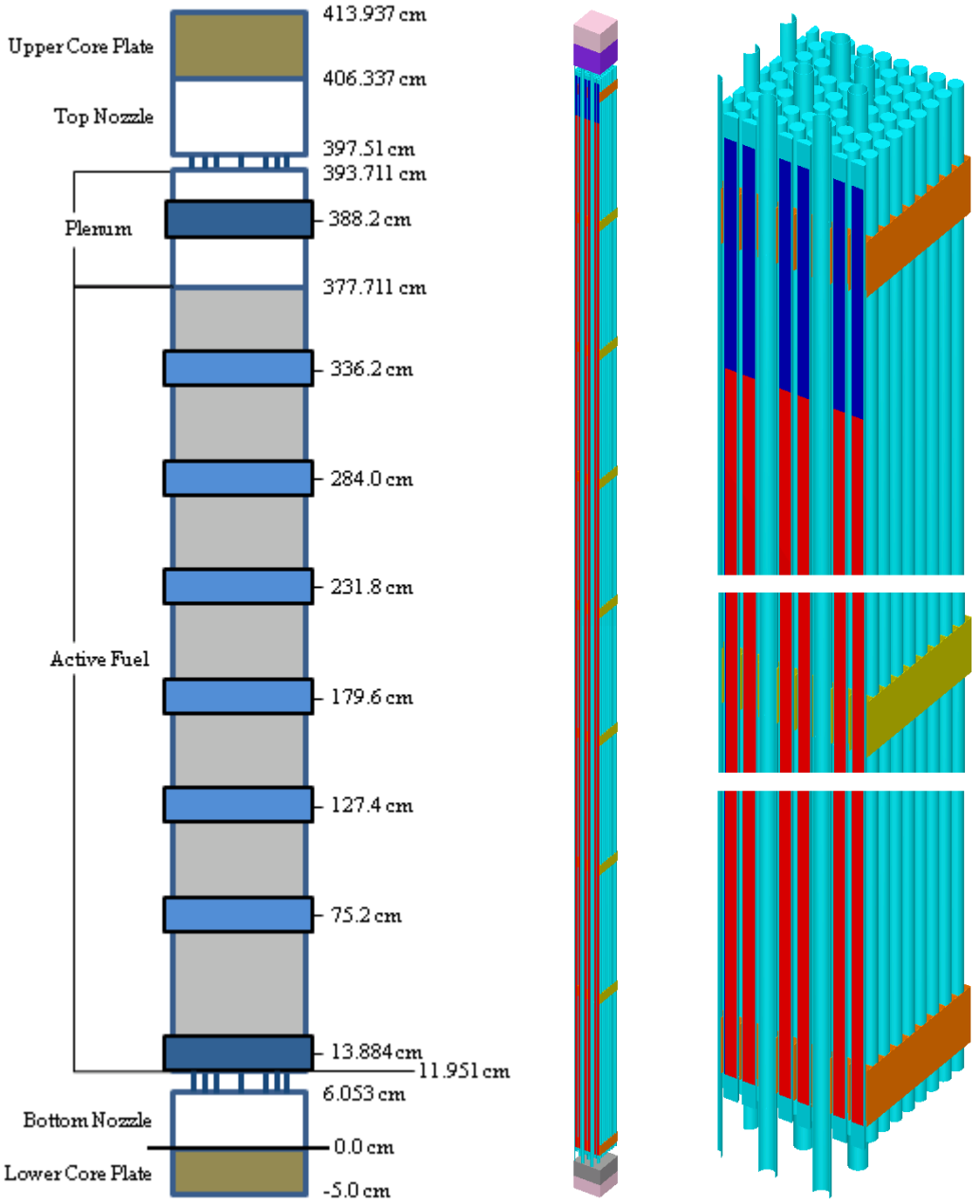

Figure P3-1. Problem 3 Axial Geometry (without end plugs) [Left], Problem 3 Reference Model [Right] (Ref. 2)

Benchmark Results

The results of the two benchmark cases for Problem 3 can be seen in Table P3-2. It can be seen that the agreement between the VERA results and those obtained using KENO is very good. Displayed are multiplication factors and differences in pin powers.

Table P3-2. Problem 3 Reference Solution Results (Ref. 2)

Problem	Description	Enrichment (%)	KENO-VI K_{eff}	VERA K_{eff}	Difference ($\Delta Kx10^5$)	Radial ΔP RMS (%)	Radial ΔP MAX (%)
3A	No Poisons	3.10	1.17572	1.17564	-9	0.08	0.16
3B	16 Pyrex	2.62	1.00015	1.00097	82	0.10	0.27

Included below are axial power distributions for the two cases. It can clearly be seen that there is good agreement axially and radially for both cases. Additionally, the axially-integrated individual pin powers are included below for both case 3A and 3B. For the axially-averaged pin powers, both the RMS and the maximum difference were very small.

For case 3A and 3B, the maximum axial power distribution RMS was found to 0.142% and 0.107% respectively, while the maximum axial power difference was found to be 0.268% and 0.353% respectively. The differences are additionally plotted in Figure P3-2 and P3-3.

Table P3-3. Problem 3 Axial Power Distribution for KENO and VERA, Bottom Portion (Ref. 2)

Level	Elevation	Thickness	KENO-VI		VERA		Difference (%)	
	(cm)	(cm)	3A	3B	3A	3B	3A	3B
0	11.951							
1	15.817	3.866	0.13945	0.16628	0.1388	0.1670	-0.065	0.072
2	24.0281	8.2111	0.19703	0.21087	0.1951	0.2093	-0.193	-0.157
3	32.2393	8.2112	0.29915	0.31134	0.2970	0.3092	-0.215	-0.214
4	40.4504	8.2111	0.39929	0.41069	0.3972	0.4090	-0.209	-0.169
5	48.6616	8.2112	0.49716	0.50769	0.4952	0.5063	-0.196	-0.139
6	56.8727	8.2111	0.59265	0.6019	0.5908	0.6008	-0.185	-0.110
7	65.0839	8.2112	0.68569	0.69336	0.6838	0.6924	-0.189	-0.096
8	73.295	8.2111	0.7682	0.77329	0.7660	0.7721	-0.220	-0.119
9	77.105	3.81	0.79068	0.78969	0.7880	0.7882	-0.268	-0.149
10	85.17	8.065	0.89182	0.89532	0.8899	0.8946	-0.192	-0.072
11	93.235	8.065	0.97853	0.98264	0.9771	0.9826	-0.143	-0.004
12	101.3	8.065	1.0527	1.05613	1.0517	1.0566	-0.100	0.047
13	109.365	8.065	1.12254	1.12492	1.1218	1.1255	-0.074	0.058
14	117.43	8.065	1.18801	1.18879	1.1871	1.1893	-0.091	0.051
15	125.495	8.065	1.23644	1.23397	1.2350	1.2340	-0.144	0.003
16	129.305	3.81	1.21448	1.20371	1.2122	1.2031	-0.228	-0.061
17	137.37	8.065	1.31438	1.31074	1.3132	1.3109	-0.118	0.016
18	145.435	8.065	1.37204	1.37027	1.3715	1.3708	-0.054	0.053
19	153.5	8.065	1.41136	1.4095	1.4113	1.4105	-0.006	0.100
20	161.565	8.065	1.44481	1.44265	1.4451	1.4435	0.029	0.085
21	169.63	8.065	1.47284	1.46893	1.4727	1.4696	-0.014	0.067
22	177.695	8.065	1.47993	1.47282	1.4794	1.4731	-0.053	0.028
23	181.505	3.81	1.41795	1.40185	1.4165	1.4014	-0.145	-0.045
24	189.57	8.065	1.49862	1.49098	1.4983	1.4912	-0.032	0.022
25	197.635	8.065	1.51653	1.51133	1.5172	1.5124	0.067	0.107

Table P3-4. Problem 3 Axial Power Distribution for KENO and VERA, Top Portion (Ref. 2)

Level	Elevation	Thickness	KENO-VI		VERA		Difference (%)	
	(cm)	(cm)	3A	3B	3A	3B	3A	3B
26	205.7	8.065	1.51357	1.50921	1.5149	1.5106	0.133	0.139
27	213.765	8.065	1.50467	1.50024	1.5062	1.5016	0.153	0.136
28	221.83	8.065	1.48986	1.48459	1.4911	1.4856	0.124	0.101
29	229.895	8.065	1.45468	1.44648	1.4554	1.4472	0.072	0.072
30	233.705	3.81	1.36407	1.34781	1.3638	1.3475	-0.027	-0.031
31	241.77	8.065	1.41065	1.40262	1.4115	1.4032	0.085	0.058
32	249.835	8.065	1.38579	1.38059	1.3875	1.3819	0.171	0.131
33	257.9	8.065	1.34148	1.33725	1.3436	1.3388	0.212	0.155
34	265.965	8.065	1.29183	1.28808	1.2940	1.2896	0.217	0.152
35	274.03	8.065	1.23691	1.23312	1.2388	1.2341	0.189	0.098
36	282.095	8.065	1.1657	1.16009	1.1670	1.1607	0.130	0.061
37	285.905	3.81	1.06292	1.05119	1.0633	1.0510	0.038	-0.019
38	293.97	8.065	1.06708	1.06193	1.0682	1.0625	0.112	0.057
39	302.035	8.065	1.00378	1.00166	1.0056	1.0024	0.182	0.074
40	310.1	8.065	0.92588	0.92521	0.9279	0.9259	0.202	0.069
41	318.165	8.065	0.84438	0.84472	0.8463	0.8451	0.192	0.038
42	326.23	8.065	0.75936	0.76009	0.7610	0.7602	0.164	0.011
43	334.295	8.065	0.66502	0.66528	0.6662	0.6650	0.118	-0.028
44	338.105	3.81	0.56887	0.56589	0.5692	0.5650	0.033	-0.089
45	346.0262	7.9212	0.53052	0.53161	0.5312	0.5309	0.068	-0.071
46	353.9474	7.9212	0.44235	0.44547	0.4430	0.4446	0.065	-0.087
47	361.8686	7.9212	0.34668	0.35096	0.3472	0.3500	0.052	-0.096
48	369.7898	7.9212	0.24941	0.25469	0.2497	0.2535	0.029	-0.119
49	377.711	7.9212	0.17166	0.18312	0.1717	0.1796	0.004	-0.352

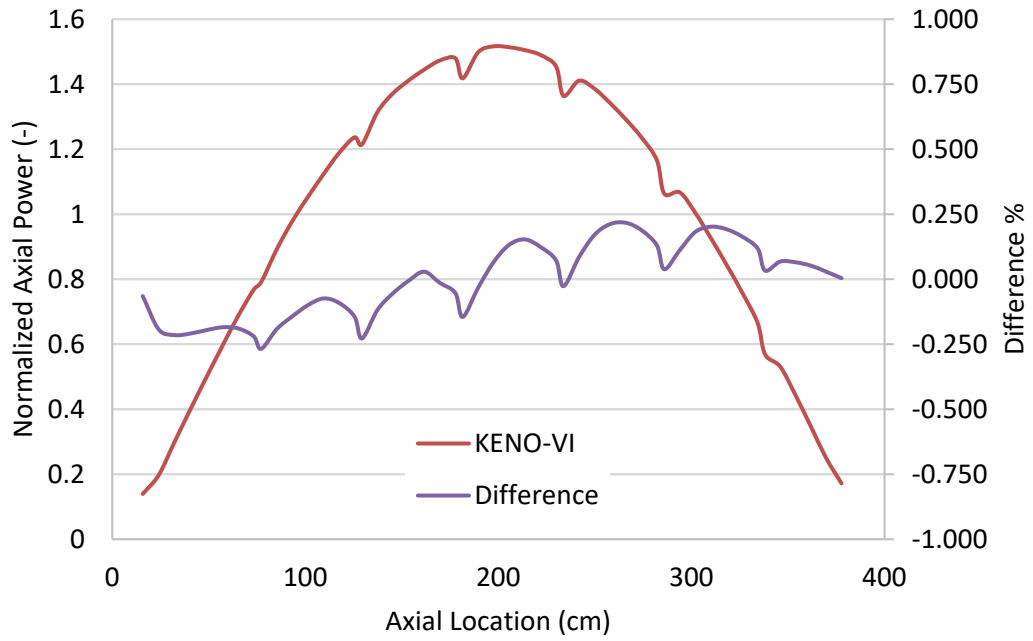

Figure P3-2. Problem 3A Normalized Axial Power and Associated Difference for VERA Results (Ref. 2)

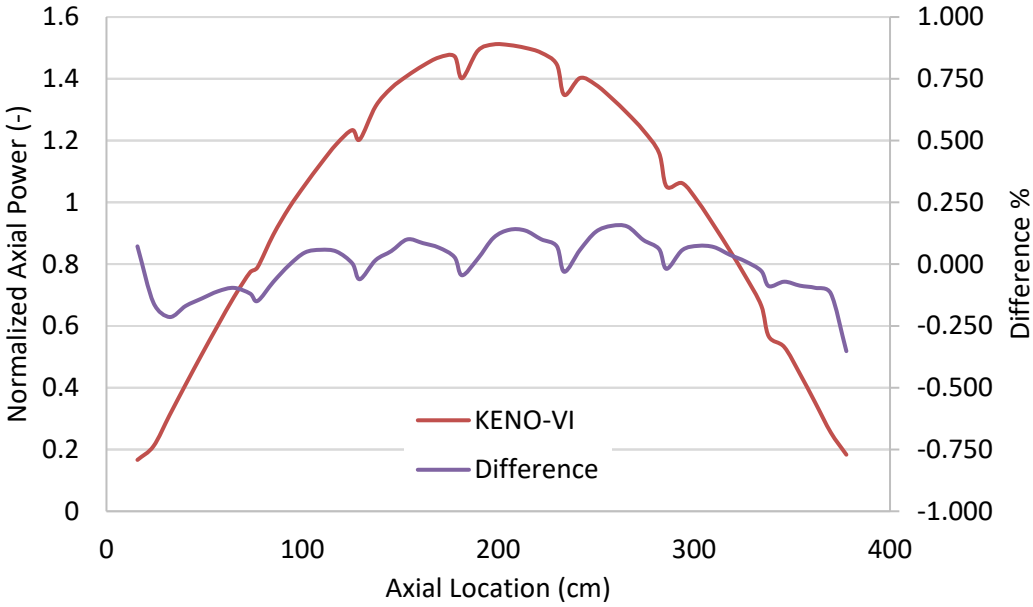

Figure P3-3. Problem 3A Normalized Axial Power and Associated Difference for VERA Results (Ref. 2)

1.0356	1.0096							
1.0363	1.0100	1.0107						
	1.0365	1.0382						
1.0349	1.0091	1.0117	1.0443	1.0317				
1.0318	1.0061	1.0091	1.0443	1.0500				
	1.0256	1.0271		1.0350	1.0166	0.9739		
1.0112	0.9883	0.9884	1.0109	0.9835	0.9656	0.9491	0.9398	
0.9771	0.9729	0.9724	0.9746	0.9655	0.9559	0.9468	0.9426	0.9479

KENO-VI (Ref. 2)

1.0346	1.0101							
1.0356	1.0110	1.0108						
	1.0360	1.0366						
1.0337	1.0089	1.0116	1.0430	1.0332				
1.0306	1.0064	1.0099	1.0427	1.0503				
	1.0241	1.0262		1.0352	1.0163	0.9742		
1.0103	0.9891	0.9894	1.0108	0.9837	0.9645	0.9497	0.9409	
0.9767	0.9731	0.9731	0.9748	0.9661	0.9564	0.9475	0.9436	0.9489

VERA

-0.10	0.05							
-0.07	0.10	0.01						
	-0.05	-0.16						
-0.12	-0.02	-0.01	-0.13	0.15				
-0.12	0.03	0.08	-0.16	0.03				
	-0.15	-0.09		0.02	-0.03	0.03		
-0.09	0.08	0.10	-0.01	0.02	-0.11	0.06	0.11	
-0.04	0.02	0.07	0.02	0.06	0.05	0.07	0.10	0.10

Difference (%)

Figure P3-4. Problem 3A Benchmark Results (Octant Symmetry), Showing KENO-VI, VERA and Percent Differences of Assembly Pin Powers

1.0531	1.0276							
0.9586	0.9945	1.0247						
	0.9568	1.0462						
0.9590	0.9934	1.0174	1.0247	0.9648				
1.0573	1.0285	0.9851	0.9229	0.8884				
	1.0628	0.9560		0.8894	0.9077	0.9666		
1.0933	1.0538	0.9987	0.9394	0.9640	0.9853	1.0111	1.0348	
1.0718	1.0580	1.0331	1.0105	1.0125	1.0231	1.0391	1.0554	1.0729

KENO-VI (Ref. 2)

1.0525	1.0275							
0.9594	0.9942	1.0241						
	0.9578	1.0453						
0.9594	0.9920	1.0170	1.0244	0.9655				
1.0565	1.0282	0.9850	0.9246	0.8902				
	1.0615	0.9567		0.8910	0.9104	0.9665		
1.0908	1.0533	0.9982	0.9407	0.9633	0.9852	1.0111	1.0347	
1.0698	1.0566	1.0326	1.0114	1.0127	1.0232	1.0389	1.0551	1.0721

VERA

-0.06	-0.01							
0.08	-0.03	-0.06						
	0.10	-0.09						
0.04	-0.14	-0.04	-0.03	0.07				
-0.08	-0.03	-0.01	0.17	0.18				
	-0.13	0.07		0.16	0.27	-0.01		
-0.25	-0.05	-0.05	0.13	-0.07	-0.01	0.00	-0.01	
-0.20	-0.14	-0.05	0.09	0.02	0.01	-0.02	-0.03	-0.08

Difference (%)

Figure P3-5. Problem 3B Benchmark Results (Octant Symmetry), Showing KENO-VI, VERA and Percent Differences of Assembly Pin Powers

PROBLEM #4: 3D HZP 3X3 ASSEMBLY CONTROL ROD WORTH

Description and Specifications

The fourth VERA core physics benchmark progression problem consists of nine Westinghouse 17x17-type fuel assemblies arranged in a 3x3. The fuel is at beginning-of-life (BOL) and Hot Zero Power (HZP) isothermal conditions. In addition to the same materials as Problem 3, this problem also tests the ability to define and place Pyrex (1.5), AIC, and B_4C (1.6) absorbers in the assembly guide tubes, as well as position the RCCA by simply providing the number of steps withdrawn for the bank. (Ref. 2)

Figure P4-1 provides the loading pattern for this problem In this figure, Region 1 is represented by the 2.11% enrichment with center RCCA, and Region 2 is the 2.619% enriched region with 20 Pyrex rods. The hybrid AIC/B_4C RCCA is located in the center assembly. This problem is ideally run in quarter or octant symmetry. (Ref. 2)

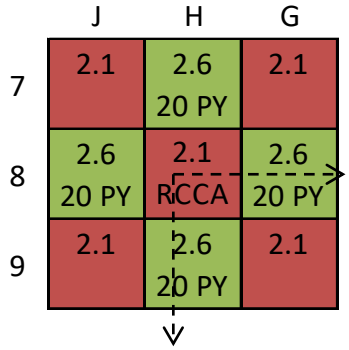

Figure P4-1. Problem 4 Assembly, Poison, and Control Layout (Ref. 2)

The reference cases for Problem 4 involve a series of different control rod positions. The first case has the bottom of the RCCA poison at a discrete position of 259.7 cm, relative to the top of the bottom core plate. The problem specification are detailed in Table P4-1. (Ref. 2)

Table P4-1. Problem 4 Specification (Ref. 2)

Input	Value
Fuel Density	10.257 g/cc
Fuel Enrichment – Region 1	2.11%
Fuel Enrichment – Region 2	2.619%
Power	0% FP
Inlet Coolant Temperature	565 K
Inlet Coolant Density	0.743 g/cc
Reactor Pressure	2250 psia
Boron Concentration	1360 ppm

Benchmark Results

The eigenvalues calculated by VERA and relevant CE KENO-VI for the reference cases are provided below. It can be seen in Table P4-2 that the difference between VERA and KENO-VI is never greater than 48pcm. The values calculated by VERA are consistently near 40 pcm higher than those calculated by KENO-VI.

Table P4-2. Problem 4 Benchmark Problem Results Comparing VERA and KENO (Ref. 2)

Rod Position	KENO-VI K_{eff}	VERA K_{eff}	Difference ($\Delta Kx10^5$)
257.9 cm	0.99898	0.99939	41
0 Steps	0.97241	0.97287	46
23 Steps	0.97368	0.97414	46
16 Steps	0.97936	0.97969	33
69 Steps	0.98704	0.98748	44
92 Steps	0.99234	0.99282	48
115 Steps	0.99574	0.99620	46
138 Steps	0.99803	0.99844	41
161 Steps	0.99955	0.99992	37
184 Steps	1.00058	1.00097	39
207 Steps	1.00117	1.00161	44
230 Steps	1.00138	1.00179	41

The differential (DRW) and integral (IRW) control rod reactivity worths were calculated by:

$$\rho_{CRD} = \left({}^{1}/_{k_{UNC}} - {}^{1}/_{k_{CON}}\right) \times 10^5 \ \ [pcm]$$

Resulting differential rod worth (DRW) and integral rod worth (IRW) are compared in Table P4-3 for KENO-VI and P4-4 for VERA. It can be seen that the IRW for both codes is very similar, differing no more than 10 pcm. Similar agreement was seen for the DRW. Additionally, both DRW and IRW are plotted for the purposes of visualization in Figure P4-2 and P4-3.

Table P4-3. Problem 4 DRW and IRW for KENO-VI (Ref. 2)

Rod Position	% Withdrawn	K-effective	DRW (pcm)	IRW (pcm)
257.9 cm	--	0.998981	--	-240
0 steps	0%	0.972411	-134	-2975
23 steps	10%	0.973679	-596	-2842
46 steps	20%	0.979363	-794	-2245
69 steps	30%	0.987043	-541	-1451
92 steps	40%	0.992341	-344	-910
115 steps	50%	0.995745	-230	-566
138 steps	60%	0.998028	-153	-336
161 steps	70%	0.999551	-103	-183
184 steps	80%	1.000584	-58	-80
207 steps	90%	1.001168	-22	-22
230 steps	100%	1.001385	--	--

Table P4-4. Problem 4 DRW and IRW for VERA

Rod Position	% Withdrawn	K-effective	DRW (pcm)	IRW (pcm)
257.9 cm	--	0.9993881	--	-240
0 steps	0%	0.9728667	-134	-2968
23 steps	10%	0.9741392	-582	-2834
46 steps	20%	0.979694	-805	-2252
69 steps	30%	0.9874842	-545	-1446
92 steps	40%	0.9928244	-342	-902
115 steps	50%	0.9962043	-224	-560
138 steps	60%	0.9984353	-149	-336
161 steps	70%	0.9999232	-105	-187
184 steps	80%	1.0009729	-63	-82
207 steps	90%	1.0016083	-18	-18
230 steps	100%	1.0017918	--	--

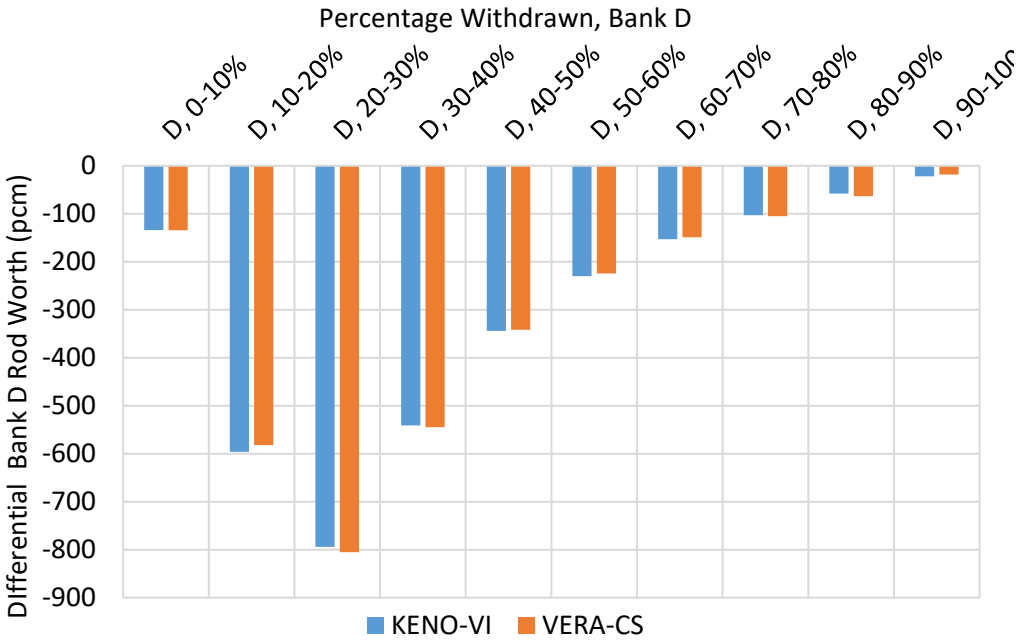

Figure P4-1. Problem 4 Differential Rod Worths for KENO-VI and VERA (Ref. 2)

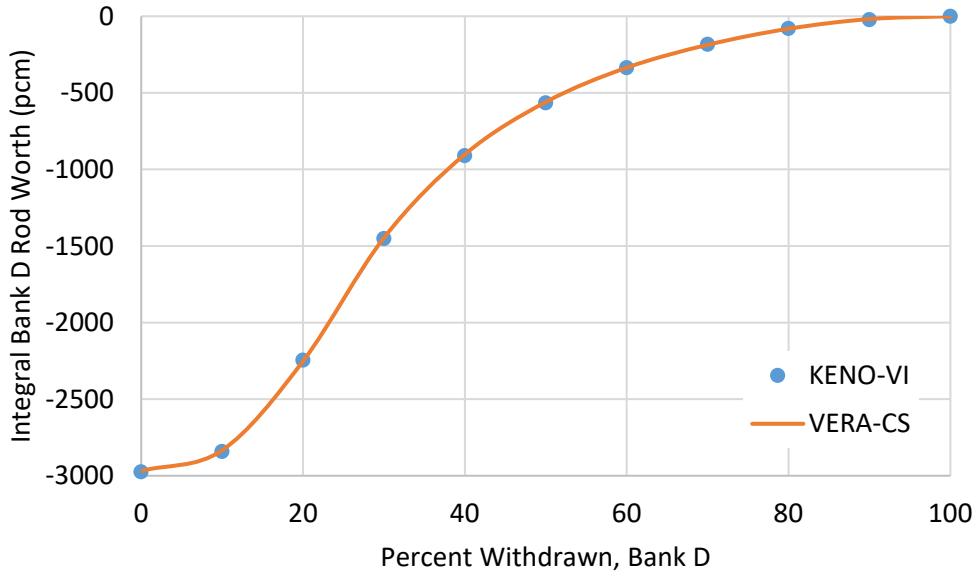

Figure P4-2. Problem 4 Integral Rod Worths for KENO-VI and VERA (Ref. 2)

PROBLEM #5: PHYSICAL REACTOR ZERO POWER PHYSICS TESTS

Description and Specifications

The fifth VERA core physics benchmark progression problem expands the test suite to a full reactor model consistent with typical nuclear core analysis. The problem consists of a full core of Westinghouse 17x17-type fuel assemblies in the WBN1 initial loading pattern. All fuel is at beginning-of-life (BOL) and Hot Zero Power (HZP) isothermal conditions. Figure P5-1 provides the loading pattern for this problem, as described in Godfrey (2014). In this figure, Region 1 is represented by the 2.11% enrichment, Region 2 is the 2.619% enriched region, and Region 3 is 3.10% enriched. (Ref. 2)

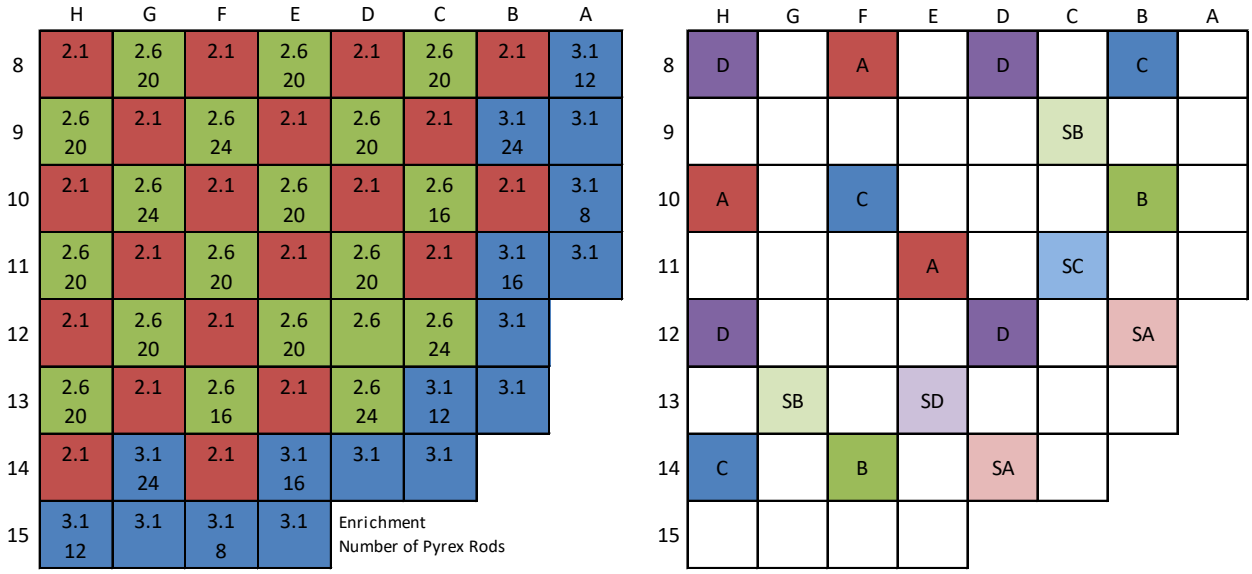

Figure P5-1. Problem 5 Assembly, Poison, and Control Rod Layout, (Quarter Symmetry) (Ref. 2)

The reference cases for Problem 5 are a variety of different control rod bank positions, soluble boron concentrations, and temperatures consistent with the actual WBN1 Cycle 1 ZPPTs. The detailed specification for the cases is provided in Table P5-2. (Ref. 2)

Table P5-1. Problem 5 Cases for WBN1 ZPPT (Ref. 2)

Bank Position (steps withdrawn)*												
Case	**Boron (ppm)**	**Temp (K)**	**A**	**B**	**C**	**D**	**SA**	**SB**	**SC**	**SD**	**Description**	
1	1285	565	-	-	-	167	-	-	-	-	Initial	**Criticals**
2	1291	↓	-	-	-	-	-	-	-	-	ARO	
3	1170	↓	0	-	-	97	-	-	-	-	Bank A	
4	↓	↓	-	0	-	113	-	-	-	-	Bank B	
5	↓	↓	-	-	0	119	-	-	-	-	Bank C	
6	↓	↓	-	-	-	18	-	-	-	-	Bank D	
7	↓	↓	-	-	-	69	0	-	-	-	Bank SA	
8	↓	↓	-	-	-	134	-	0	-	-	Bank SB	
9	↓	↓	-	-	-	71	-	-	0	-	Bank SC	
10	↓	↓	-	-	-	71	-	-	-	0	Bank SD	
11	↓	↓	-	-	-	-	-	-	-	-	ARO	**Rod Worths**
12	↓	↓	0	-	-	-	-	-	-	-	Bank A	
13	↓	↓	-	0	-	-	-	-	-	-	Bank B	
14	↓	↓	-	-	0	-	-	-	-	-	Bank C	
15	↓	↓	-	-	-	0	-	-	-	-	Bank D	
16	↓	↓	-	-	-	-	0	-	-	-	Bank SA	
17	↓	↓	-	-	-	-	-	0	-	-	Bank SB	
18	↓	↓	-	-	-	-	-	-	0	-	Bank SC	
19	↓	↓	-	-	-	-	-	-	-	0	Bank SD	
20	1291	560	-	-	-	-	-	-	-	-	Low temp	**ITC**
21	↓	570	-	-	-	-	-	-	-	-	High temp	
22	1230	565	-	-	-	0	-	-	-	-	D @ 0%	**Bank D Integral Worth**
23	↓	↓	-	-	-	23	-	-	-	-	D @ 10%	
24	↓	↓	-	-	-	46	-	-	-	-	D @ 20%	
25	↓	↓	-	-	-	69	-	-	-	-	D @ 30%	
26	↓	↓	-	-	-	92	-	-	-	-	D @ 40%	
27	↓	↓	-	-	-	115	-	-	-	-	D @ 50%	
28	↓	↓	-	-	-	138	-	-	-	-	D @ 60%	
29	↓	↓	-	-	-	161	-	-	-	-	D @ 70%	
30	↓	↓	-	-	-	184	-	-	-	-	D @ 80%	
31	↓	↓	-	-	-	207	-	-	-	-	D @ 90%	
32	↓	↓	-	-	-	-	-	-	-	-	D @ 100%	

*Fully withdrawn banks (230 steps) are indicated with a dash (-)

Benchmark Results

Benchmark results for the VERA software can be seen in Table P5-2. It can be seen that the reactivity difference is no greater than 35 pcm for any of the 32 separate cases found within this problem. Like in Problem 4, it can be seen that the difference is consistently higher for VERA, by ~30 pcm compared to ~40 pcm for Problem 4.

Table P5-2. Problem 5 Benchmark Results for WBN1 ZPPT (Ref. 2)

Case	Boron (ppm)	Temp. (K)	Description	KENO-VI K_{eff}	VERA K_{eff}	Difference ($\Delta Kx10^5$)	
1	1285	565	Initial	0.99990	1.00021	31	Criticals
2	1291	↓	ARO	1.00032	1.00064	32	
3	1170	↓	Bank A	0.99880	0.99906	26	
4	↓	↓	Bank B	0.99936	0.99959	23	
5	↓	↓	Bank C	0.99904	0.99931	27	
6	↓	↓	Bank D	0.99908	0.99941	33	
7	↓	↓	Bank SA	0.99902	0.99926	24	
8	↓	↓	Bank SB	0.99932	0.99964	31	
9	↓	↓	Bank SC	0.99898	0.99928	29	
10	↓	↓	Bank SD	0.99898	0.99928	30	
11	↓	↓	ARO	1.01284	1.01313	29	Rod Worths
12	↓	↓	Bank A	1.00372	1.00400	28	
13	↓	↓	Bank B	1.00394	1.00425	31	
14	↓	↓	Bank C	1.00284	1.00313	29	
15	↓	↓	Bank D	0.99882	0.99915	33	
16	↓	↓	Bank SA	1.00828	1.00857	29	
17	↓	↓	Bank SB	1.00202	1.00234	32	
18	↓	↓	Bank SC	1.00775	1.00805	30	
19	↓	↓	Bank SD	1.00774	1.00805	31	
20	1291	560	Low temp	1.00061	1.00095	35	ITC
21	↓	570	High temp	1.00003	1.00037	34	
22	1230	565	D @ 0%	0.99276	0.99309	33	Bank D Integral Worth
23	↓	↓	D @ 10%	0.99316	0.99349	33	
24	↓	↓	D @ 20%	0.99456	0.99488	32	
25	↓	↓	D @ 30%	0.99737	0.99770	33	
26	↓	↓	D @ 40%	1.00028	1.00062	34	
27	↓	↓	D @ 50%	1.00254	1.00287	32	
28	↓	↓	D @ 60%	1.00416	1.00448	32	
29	↓	↓	D @ 70%	1.00530	1.00560	30	
30	↓	↓	D @ 80%	1.00607	1.00636	29	
31	↓	↓	D @ 90%	1.00647	1.00679	32	
32	↓	↓	D @ 100%	1.00658	1.00690	31	

The criticals for Problem 5 are shown in Figure P5-2. It can be seen that VERA consistently predicts values higher than KENO-VI. For the criticals themselves, which have an empirical value of 1.0000,

the VERA code provides a closer prediction than KENO-VI. The average is 0.99957 for VERA compared to 0.99928 for KENO.

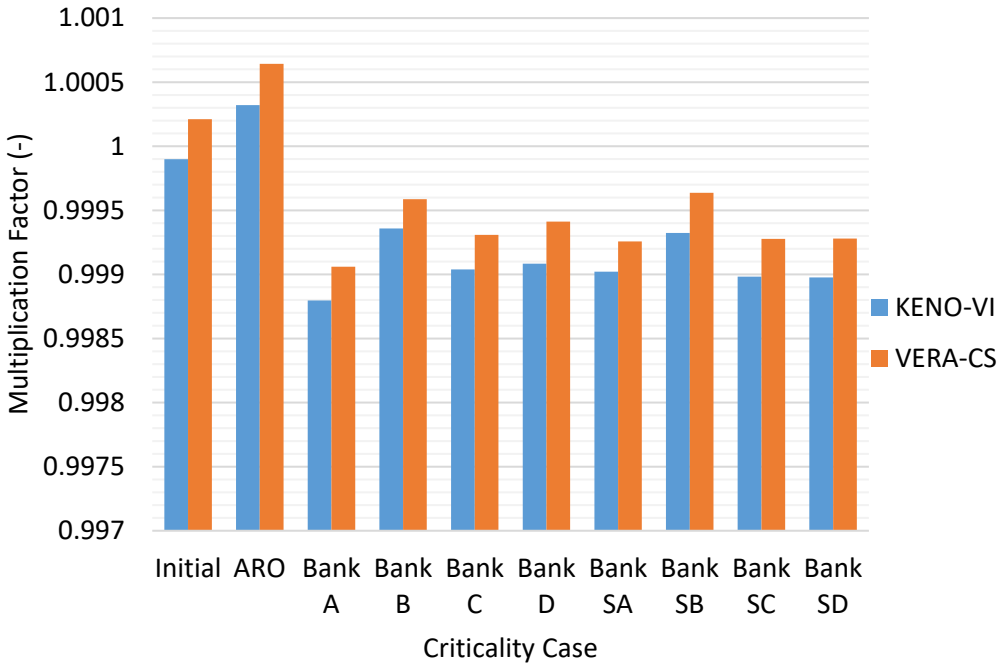

Figure P5-2. Problem 5 Benchmark Solution Criticals (Ref. 2)

The ZPPT control bank worths, differential boron worth, and isothermal temperature coefficient were calculated and provided in the table below using the following equation for reactivity difference:

$$\rho = \left({}^{1}/_{k_1} - {}^{1}/_{k_2}\right) \times 10^5 \ \ [pcm]$$

It can be seen that VERA agrees well with KENO-VI and measured data for the both the DRW and IRW calculations. The largest differences for both codes compared to measured data is for Bank A, which shows both codes over predicting worth by 6.4%. IRW and DRW are presented graphically in Figure P5-3 and P5-4 for the purposes of visualization. The only difference of note is that the isothermal temperature coefficient (ITC) is significantly more negative than the measured plant value. However, differential boron reactivity worth (DBW) shows good agreement.

Table P5-7. Problem 5 Measured and Reference Solution ZPPT Results (Ref. 2)

Test Result	Measured	Keno-VI		VERA	
		Results	Difference	Results	Difference
Initial Criticality	1.00000	0.99990	-10 pcm	1.00021	21 pcm
Bank A Worth (pcm)	843	898	6.4 %	898	6.4 %
Bank B Worth (pcm)	879	875	-0.5 %	873	-0.7 %
Bank C Worth (pcm)	951	984	3.5 %	984	3.4 %
Bank D Worth (pcm)	1342	1386	3.3 %	1381	2.9 %
Bank SA Worth (pcm)	435	447	2.6 %	446	2.6 %
Bank SB Worth (pcm)	1056	1066	1.0 %	1063	0.6 %
Bank SC Worth (pcm)	480	499	3.9 %	497	3.6 %
Bank SD Worth (pcm)	480	499	4.0 %	497	3.5 %
Total Bank Worths (pcm)	6467	6654	2.9 %	6639	2.7 %
DBW (pcm)	-10.77	-10.21	0.56	-10.34	0.43
ITC (pcm)	-2.17	-3.18	-1.01	-3.22	-1.05

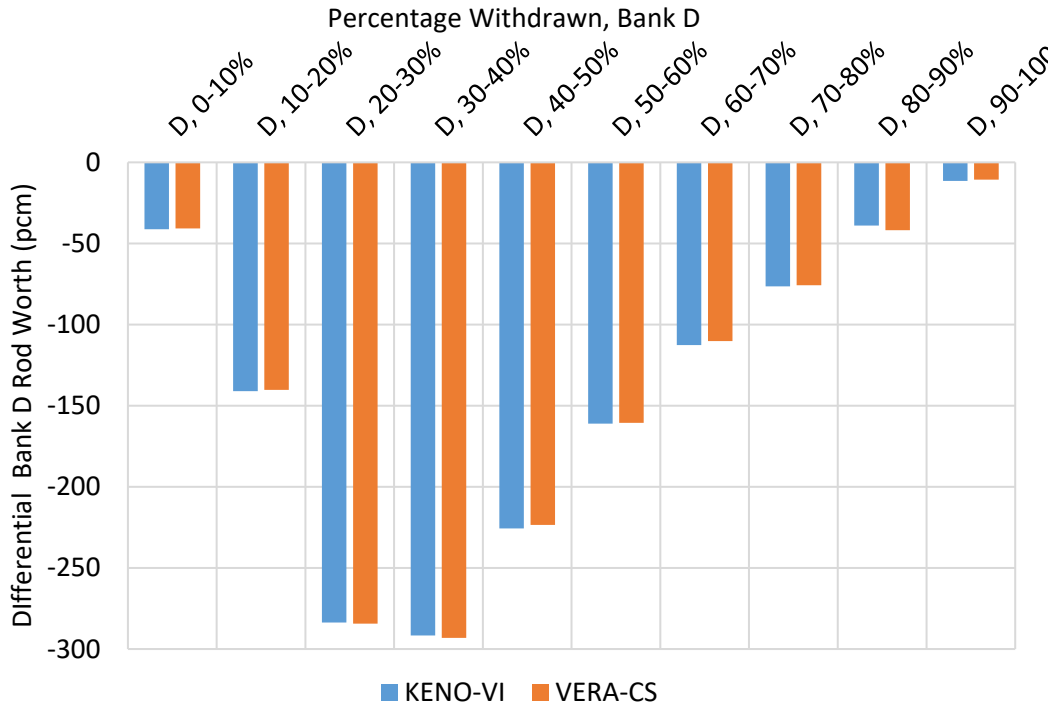

Figure P5-3. Problem 5 Bank D Differential Worths for KENO-VI and VERA (Ref. 2)

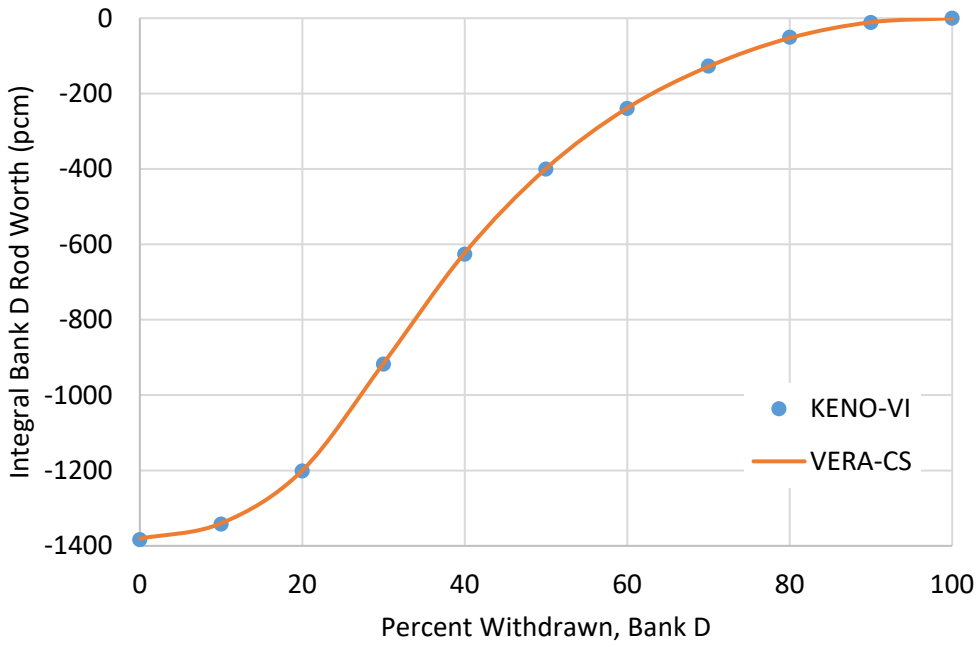

Figure P5-4. Problem 5 Bank D Integral Rod Worths for KENO-VI and VERA (Ref. 2)

The individual pin powers for this analysis are too large to include in this document. However, assembly-averaged powers are displayed for a "base" case that did not include the incore instrument thimbles in order to maintain octant symmetry and produce lower power distribution uncertainties. Otherwise, it is the same as Case 5A. The eigenvalue for this case is 1.00007 ± 0.000002 for the KENO-VI reference and 1.00047 for VERA. The axially-averaged radial assembly power RMS for the case is 0.23%, and the maximum power difference is 0.53%.

0.9487					
0.9193	0.9973				
1.0181	0.9083	1.0648			
0.9850	1.0819	1.0412	1.1615		
1.0647	1.0471	1.1746	1.0850	1.2368	
1.0480	1.1619	1.152	1.1508	0.8969	0.9126
1.0841	1.0652	1.1039	1.0496	0.9452	0.6296
0.7931	0.9071	0.8046	0.6590		

KENO-VI (Ref. 2)

0.9518					
0.9246	0.9998				
1.0200	0.9122	1.0649			
0.9882	1.0818	1.0428	1.1588		
1.0636	1.0483	1.1716	1.0845	1.2341	
1.0487	1.1586	1.1506	1.1463	0.8964	0.9135
1.0810	1.0658	1.0993	1.0492	0.9458	0.6318
0.7955	0.9088	0.8057	0.6601		

VERA

0.31					
0.53	0.25				
0.19	0.39	0.01			
0.32	-0.01	0.16	-0.27		
-0.11	0.12	-0.30	-0.05	-0.27	
0.07	-0.33	-0.14	-0.45	-0.05	0.09
-0.31	0.06	-0.46	-0.04	0.06	0.22
0.24	0.17	0.11	0.11		

Difference (%)

Figure P5-5. Problem 5 KENO-VI, VERA and Associated Differences for Radial Assembly Powers (Octant Symmetry)

It can be seen that there is good agreement in Figure P5-6, when comparing pin power within the whole reactor core, despite a slightly differing scale in the two diagrams.

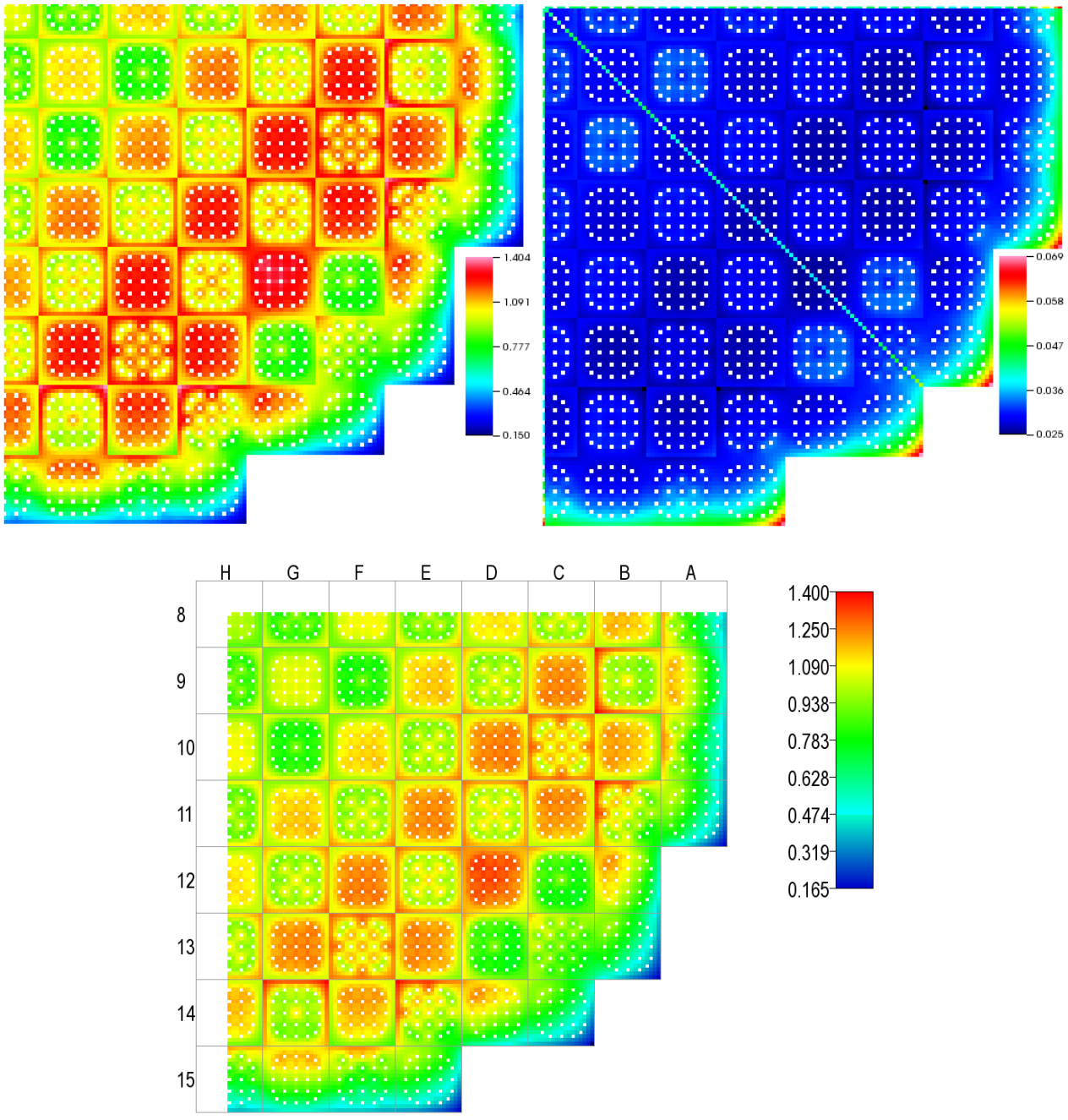

Figure P5-5. Problem 5 [TOP] CE KENO-VI Radial Power Distribution and Uncertainty (%), [Bottom] VERA (Ref. 2)

PROBLEM #6: 3D HFP ASSEMBLY

Description and Specifications

This core physics benchmark problem demonstrates VERA's performance for an operating reactor condition requiring a coupled multi-physics iterative solution. The geometry is a single PWR fuel assembly identical to Problem 3. However, this assembly is at typical full power and nominal flow conditions, requiring the additional capability of thermal-hydraulic feedback to the neutronics in both the fuel and coolant properties. (Ref. 2)

The problem geometry is identical to Problem 3 (3A) and consists of a single Westinghouse 17x17-type fuel assembly at beginning-of-life (BOL) and Hot Full Power (HFP) conditions, based on WBN1 data. The materials are standard for this type of reactor. The moderator contains soluble boron as a chemical shim for maintaining criticality. The focus of this problem is to demonstrate the ability to provide the neutronics with thermal-hydraulic feedback. Table P6-1 provides the problem specifications. (Ref. 2)

Table P6-1. Problem 6 Specification (Ref. 2)

Input	Value
Fuel Density	10.257 g/cc
Fuel Enrichment	3.1%
Inlet Coolant Temperature	565 K
Reactor Pressure	2250 psia
Boron Concentration	1300 ppm
Rated Power (100%)	17.67 MW
Rated Coolant Mass Flow (100%)	0.6823 Mlbs/hr

Unlike Benchmark Progression Problems 1 through 5, the reference solution for this problem was provided by a coupled MC21/CTF analysis. This reference solution and another in-depth benchmark against VERA can be seen in Kelly et al. (2017).

Benchmark Results

Key results for the benchmark problem can be seen in Table P6-2.It can be seen that there is good agreement between both the multiplication factor and the axially-integrated pin powers calculated by the two coupled code systems. VERA predicts a lower multiplication factor by 63 pcm. The radial pin power RMS is less than 0.1%, while the maximum pin power difference is less than 0.2%. Differences between this benchmark and the one performed in Kelly et al. (2017) can be attributed to different working builds of the software.

Table P6-2. Problem 6, Key Benchmark Results, Comparing Multiplication Factors and Pin Powers Differences (Ref. 6)

MC21/CTF (K_{eff})	VERA (K_{eff})	Reactivity Difference (ΔKx10^5)	Radial ΔP RMS (%)	Radial ΔP MAX (%)
1.16424	1.16361	-63	0.08	-0.19

Pin powers for both VERA and MC1/CTF can be seen in Figure P6-1. The largest pin power differences, though still small in magnitude, are found within the center of the assembly, likely caused by proximity to water rods. A three dimensional visualization of local power within the assembly can

be seen in Figure P6-2. It can be seen that the power in concentrated in the central region of the assembly.

	1.0373	1.0372		1.0354	1.0323		1.0122	0.9768
1.0373	1.0098	1.0099	1.0372	1.0085	1.0056	1.0259	0.9880	0.9725
1.0372	1.0100	1.0106	1.0387	1.0112	1.0086	1.0275	0.9880	0.9718
	1.0373	1.0388		1.0448	1.0450		1.0114	0.9740
1.0354	1.0085	1.0112	1.0450	1.0318	1.0512	1.0362	0.9832	0.9649
1.0324	1.0056	1.0085	1.0451	1.0511		1.0173	0.9647	0.9553
	1.0262	1.0275		1.0361	1.0174	0.9732	0.9479	0.9462
1.0120	0.9880	0.9882	1.0116	0.9832	0.9645	0.9479	0.9385	0.9421
0.9768	0.9725	0.9719	0.9741	0.9660	0.9555	0.9463	0.9423	0.9479

MC21/CTF (Ref. 6)

	1.0354	1.0363		1.0344	1.0313		1.0110	0.9762
1.0354	1.0099	1.0107	1.0366	1.0086	1.0061	1.0249	0.9889	0.9725
1.0363	1.0107	1.0105	1.0373	1.0113	1.0096	1.0269	0.9892	0.9724
	1.0366	1.0372		1.0438	1.0436		1.0116	0.9741
1.0344	1.0085	1.0113	1.0438	1.0336	1.0517	1.0365	0.9834	0.9654
1.0313	1.0060	1.0096	1.0436	1.0517		1.0170	0.9636	0.9556
	1.0248	1.0269		1.0365	1.0170	0.9737	0.9487	0.9467
1.0110	0.9889	0.9892	1.0116	0.9834	0.9636	0.9487	0.9400	0.9430
0.9762	0.9725	0.9724	0.9741	0.9654	0.9556	0.9467	0.9430	0.9487

VERA

	-0.19	-0.09		-0.10	-0.10		-0.12	-0.06
-0.19	0.01	0.08	-0.06	0.01	0.05	-0.10	0.09	0.00
-0.09	0.07	-0.01	-0.14	0.01	0.10	-0.06	0.12	0.06
	-0.07	-0.16		-0.10	-0.14		0.02	0.01
-0.10	0.00	0.01	-0.12	0.18	0.05	0.03	0.02	0.05
-0.11	0.04	0.11	-0.15	0.06		-0.03	-0.11	0.03
	-0.14	-0.06		0.04	-0.04	0.05	0.08	0.05
-0.10	0.09	0.10	0.00	0.02	-0.09	0.08	0.15	0.09
-0.06	0.00	0.05	0.00	-0.06	0.01	0.04	0.07	0.08

Difference (%)

Figure P6-1. Problem 6 Benchmark Results (Quadrant Symmetry), Showing MC21/CTF, VERA and Percent Differences of Radial Pin Powers

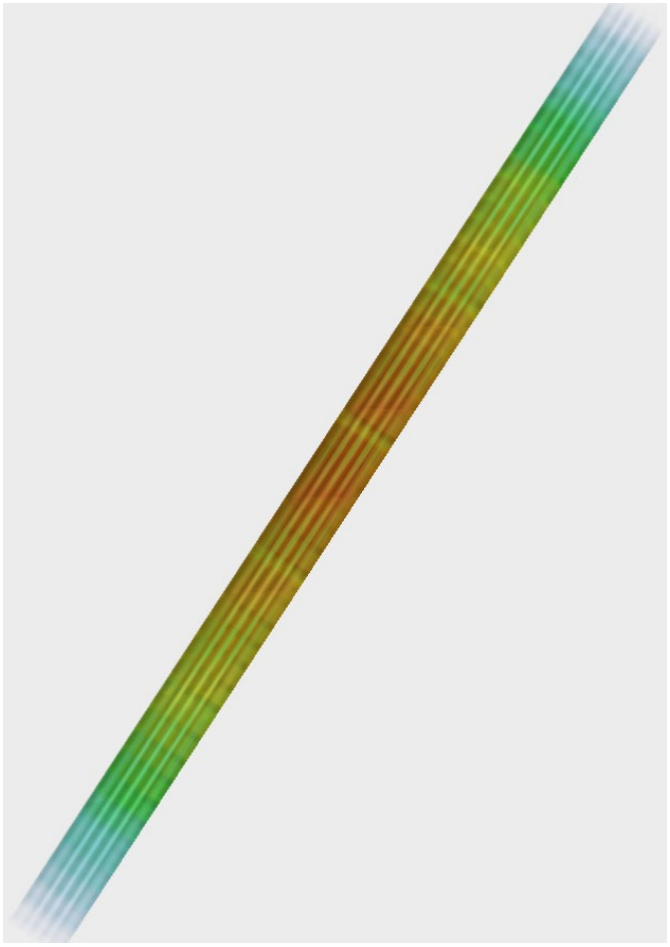

Figure P6-2. Problem 6 Visualization of Local Power Computed using VERA

PROBLEM #7: 3D HFP BOC PHYSICAL REACTOR

Description and Benchmark

This core physics benchmark problem demonstrates VERA's performance for an operating reactor in full geometric detail. The geometry is the Watts Bar Cycle 1 core identical to Problem 5. However, the problem is run a full power and nominal flow conditions, utilizing thermal-hydraulic feedback to the neutronics in both the fuel and coolant properties. Additionally this problem adds the requirements for calculation of equilibrium xenon isotopics and critical soluble boron search. (Ref. 2)

The problem geometry is identical to Problem 5 and consists of a full core of Westinghouse 17x17-type fuel assemblies in the WBN1 initial loading pattern (Sections 1.1 to 1.7 and Section 1.12). The core is at beginning-of-life (BOL) and Hot Full Power (HFP) conditions, including nominal power and flow. The RCCA banks are fully withdrawn, except for Bank D which remains slightly inserted for reactivity control. In order to properly predict a HFP power distribution, the equilibrium concentration of the fission product Xenon must be calculated and distributed correctly in each fuel rod location in the core. Finally, the code must also calculate the soluble boron concentration that keeps the reactor core critical (k-effective = 1.0). (Ref. 2)

The loading pattern and core geometry are shown in the section on Problem 5. Table P7-1 provides some additional problem specifications:

Table P7-1. Problem 7 Input Specification (Ref. 2)

Input	Value
Inlet Coolant Temperature	565 K
Reactor Pressure	2250 psia
Rated Power (100%)	3411 MW
Rated Coolant Mass Flow (100%)	131.7 Mlbs/hr
RCCA Bank D Position (steps withdrawn)	215

Unlike Benchmark Progression Problems 1 through 5, the reference solution for this problem was provided by a coupled MC21/CTF analysis. This reference solution and another in-depth benchmark against VERA can be seen in Kelly et al. (2017).

Benchmark Results

Key results for the benchmark problem can be seen in Table P7-2.It can be seen that there is good agreement between the critical boron concentrations calculated by the two coupled code systems. VERA predicts a lower concentration by only 0.8 ppm. The assembly power RMS is 0.21%, while the maximum assembly power difference is less than 0.5%.

Table P7-2. Problem 7, Key Benchmark Results, Comparing Critical Boron Concentration, Assembly Powers and Coolant Exit Temperatures (Ref. 6)

MC21/ CTF (ppm)	MPACT/ CTF (ppm)	Difference (ppm)	Assembly ΔP RMS (%)	Assembly ΔP MAX (%)	Exit Coolant Temp. RMS (K)	Max Exit Coolant Temp. Diff. (K)
854.5	853.7	-0.8	0.21	-0.47	0.15	0.32

Additionally, good agreement was found on coolant exit temperatures, with no single assembly showing a difference of more than 0.3 K. Differences between this benchmark and the one performed

in Kelly et al. (2017) can be attributed to different working builds of the software. Assembly powers can be found in Figure P7-1, while core coolant exit temperatures can be found in Figure P7-2. Shown in both figures is also the deviation between the two software programs.

1.1179	1.0302	1.1156	1.0564	1.1571	1.0531	1.0487	0.7558
1.0299	1.1081	0.9828	1.1475	1.0795	1.1549	1.0119	0.8558
1.1148	0.9825	1.1310	1.0740	1.1844	1.1210	1.0552	0.7646
1.0556	1.1471	1.0740	1.1798	1.0774	1.1184	0.9865	0.6335
1.1566	1.0793	1.1850	1.0777	1.2377	0.8650	0.8914	
1.0537	1.1557	1.1219	1.1193	0.8654	0.8656	0.6073	
1.0492	1.0128	1.0565	0.9876	0.8923	0.6077		
0.7563	0.8565	0.7653	0.6343				

MC21/CTF (Ref. 6)

1.1176	1.0326	1.1159	1.0590	1.1574	1.0547	1.0453	0.7550
1.0326	1.1090	0.9861	1.1489	1.0826	1.1547	1.0121	0.8547
1.1159	0.9861	1.1327	1.0777	1.1856	1.1225	1.0517	0.7632
1.0590	1.1489	1.0777	1.1810	1.0799	1.1165	0.9854	0.6322
1.1574	1.0826	1.1856	1.0799	1.2379	0.8640	0.8896	
1.0547	1.1547	1.1225	1.1165	0.8640	0.8631	0.6060	
1.0453	1.0121	1.0517	0.9854	0.8896	0.6060		
0.7550	0.8548	0.7632	0.6322				

VERA

-0.03	0.24	0.03	0.26	0.03	0.16	-0.34	-0.08
0.27	0.09	0.33	0.14	0.31	-0.02	0.02	-0.11
0.11	0.36	0.17	0.37	0.12	0.15	-0.35	-0.14
0.34	0.18	0.37	0.12	0.25	-0.19	-0.11	-0.13
0.08	0.33	0.06	0.22	0.02	-0.10	-0.18	
0.10	-0.10	0.06	-0.28	-0.14	-0.25	-0.13	
-0.39	-0.07	-0.48	-0.22	-0.27	-0.17		
-0.13	-0.17	-0.21	-0.21				

Difference (%)

Figure P7-1. Problem 7 Benchmark Results (Quadrant Symmetry), Showing MC21/CTF, VERA and Percent Differences of Assembly Powers

330.9	327.4	330.8	328.2	332.1	328.2	328.9	318.5
327.4	330.5	325.9	331.8	329.0	332.2	326.6	321.9
330.8	325.9	331.3	328.8	333.0	330.3	329.2	318.7
328.2	331.8	328.8	332.9	329.1	331.0	326.0	314.5
332.1	329.0	333.0	329.1	334.2	322.5	323.0	
328.2	332.2	330.3	331.1	322.6	322.1	313.6	
328.9	326.7	329.2	326.0	323.1	313.6		
318.5	321.9	318.8	314.5				

MC21/CTF (Ref. 6)

331.0	327.7	331.0	328.5	332.3	328.3	328.9	318.5
327.7	330.8	326.2	332.0	329.2	332.2	326.7	321.9
330.9	326.2	331.5	329.1	333.1	330.4	329.1	318.7
328.5	332.0	329.1	333.0	329.2	331.0	326.0	314.4
332.2	329.2	333.1	329.2	334.2	322.6	322.9	
328.3	332.2	330.4	331.0	322.6	322.0	313.5	
328.8	326.7	329.1	326.0	322.9	313.5		
318.5	321.8	318.7	314.4				

VERA

0.10	0.31	0.17	0.32	0.16	0.13	-0.04	0.00
0.30	0.25	0.27	0.20	0.24	0.04	0.14	-0.03
0.10	0.26	0.18	0.29	0.14	0.13	-0.12	0.01
0.30	0.20	0.29	0.09	0.14	-0.03	-0.04	-0.10
0.10	0.24	0.15	0.14	0.00	0.05	-0.07	
0.10	0.04	0.13	-0.12	-0.05	-0.11	-0.11	
-0.10	0.04	-0.12	-0.04	-0.17	-0.11		
0.00	-0.10	-0.09	-0.10				

Difference (ΔK)

Figure P7-2. Problem 7 Benchmark Results (Quadrant Symmetry), Showing MC21/CTF, VERA and Temperature Differences of Core Exit Coolant Temperature in Kelvin

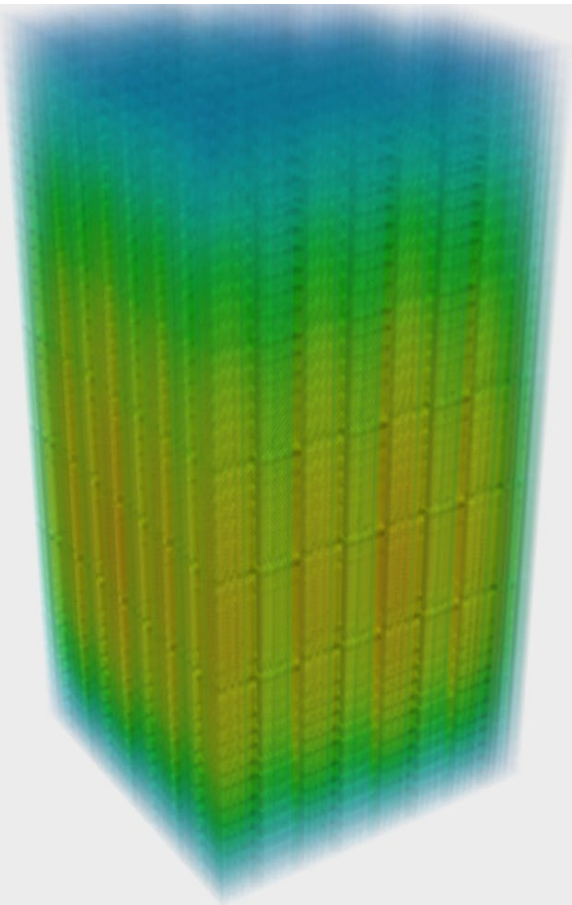

Figure P7-3. Problem 7 Visualization of Local Power Computed using VERA

A 3D visualization of local power for a quarter of the reactor core can be seen in Figure P7-3. It can be seen that higher local powers are concentrated in the central region of the reactor core, while lower powers are found on the edge of the reactor core.

A comparison of pin powers for the full reactor core can be found in Figure P7-4. Contained is a 2D pin power map for both MC21/CTF and VERA/CS.

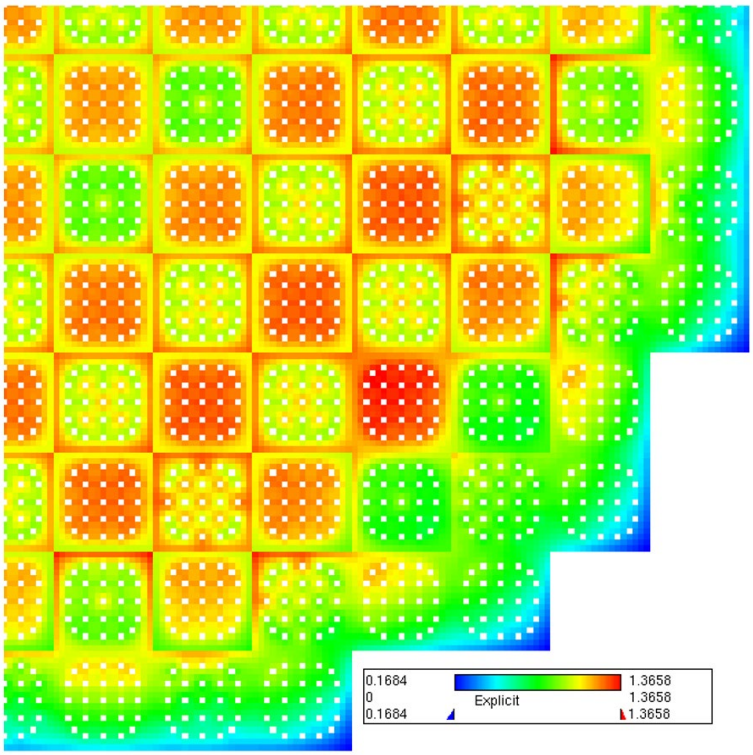

MC21/CTF (Ref. 6)

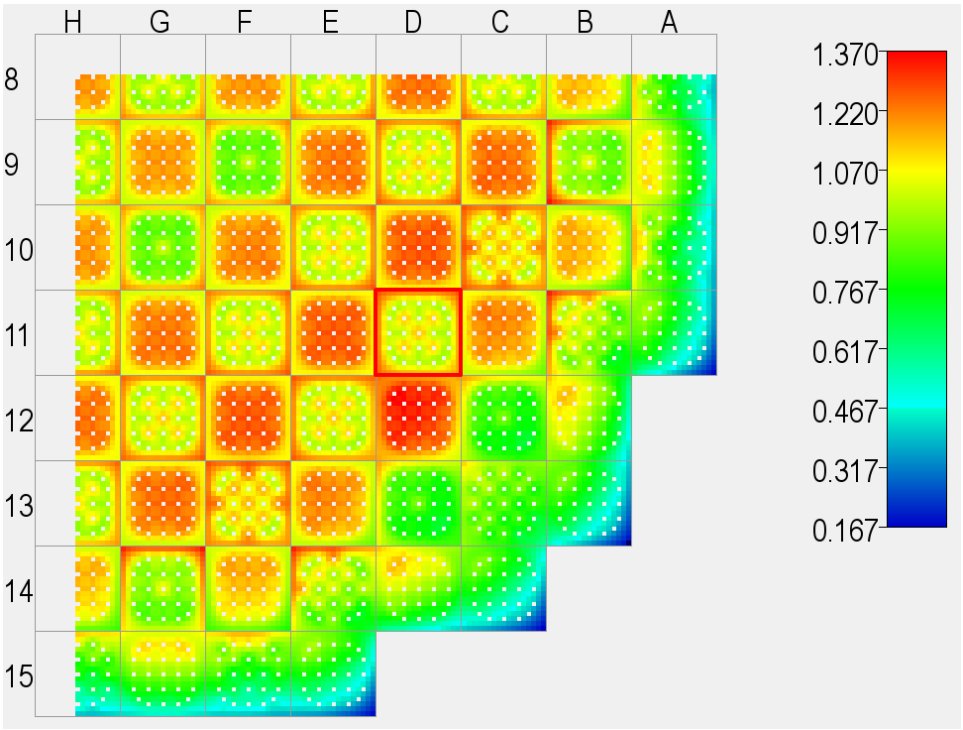

VERA

Figure P7-4. Axially-Averaged Pin Powers Computed using VERA and MC-21, (Quadrant Symmetry)

PROBLEM #8: PHYSICAL REACTOR STARTUP FLUX MAPS

Description and Specification

The geometry is equivalent to that of Problems 5 and 7. However, instead of a single statepoint at BOC HFP equilibrium conditions, a time-dependent simulation of a power escalation procedure is modeled. Included are predictions of the incore instrumentation response at various points during the startup. As with Problem 7, thermal-hydraulic feedback to the neutronics is required. Additional requirements include the calculation of transient xenon isotopics (in the absence of depletion). The WBN1C1 initial startup occurred over a very long period of initial tests, which included several planned and unplanned turbine trips and reactor shutdowns. This specification includes only a hypothetical startup procedure and will be revised at a later date when measured data is available and complete. (Ref. 2)

The core geometry and operating characteristics are the same as provided in Problems 5 and 7. Power is initially zero at BOC, fresh fuel, and no xenon conditions. Power is then increased gradually through a prescribed ramp procedure, stopping occasionally for incore flux maps and other plant procedures at specified power plateaus. For each step, the critical boron concentration is be calculated for comparison to plant data. The RCCA removal procedure is provided in Figure P8-1 and further documented in Table P8-2. (Ref. 2)

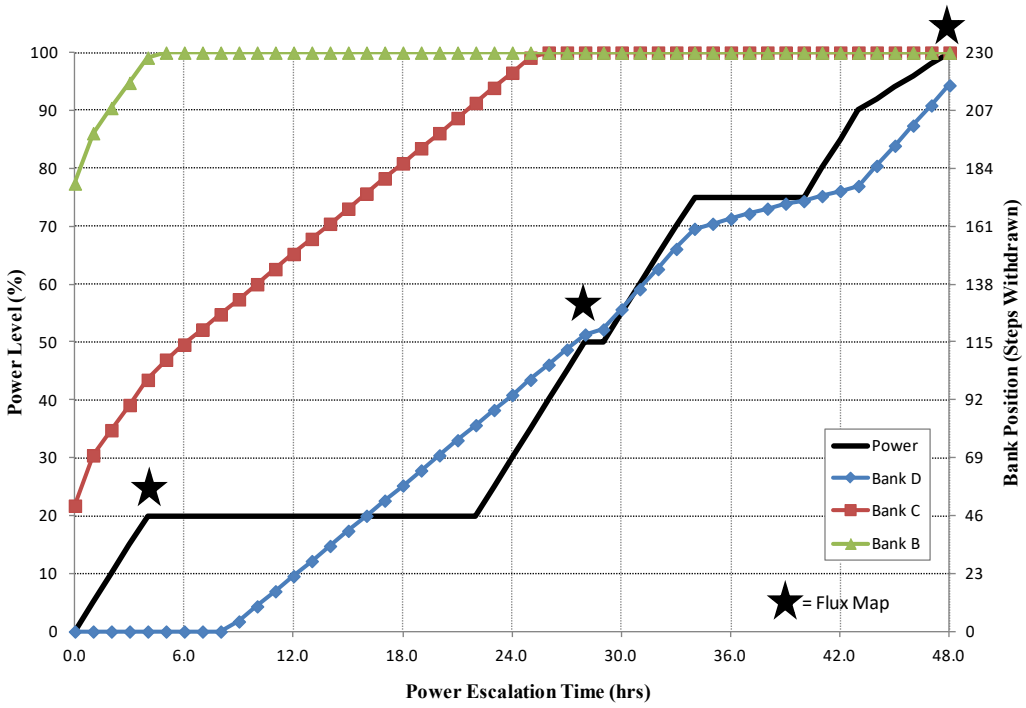

Figure P8-1. Card of Rod Removal Procedure and Reactor Power for Problem 8 (Ref. 2)

Benchmark Results

Benchmark results for the Problem 8 calculation performed in VERA are shown in Table P8-1 and Table P8-2. The computed boron concentration follows closely to the specified power ramps and rod bank withdrawals. The effect of xenon build up in the core can clearly be seen, as boron concentration decreases, in Figure P8-2, which tracks critical boron concentration against the step in the power escalation. Additionally, included in this section are assembly and radial pin power maps of the reactor core at the state points which have flux maps (5, 29 & 49). Currently this benchmark is not compared to measured data, this benchmark will be appended and included as it becomes available and/or is computed.

Table P8-1. Problem 8 Benchmark Case Results for VERA Computed Critical Boron Concentration for State Points 1-25 (Ref. 2)

Case	Hours	Power	Bank B	Bank C	Bank D	Flux Map	Computed Boron
1	0	0	178	50	0		1059
2	1	5	198	70	0		1074
3	2	10	208	80	0		1075
4	3	15	218	90	0		1073
5	4	20	228	100	0	Yes	1069
6	5	20	230	108	0		1073
7	6	20	230	114	0		1068
8	7	20	230	120	0		1064
9	8	20	230	126	0		1060
10	9	20	230	132	4		1055
11	10	20	230	138	10		1052
12	11	20	230	144	16		1048
13	12	20	230	150	22		1046
14	13	20	230	156	28		1044
15	14	20	230	162	34		1043
16	15	20	230	168	40		1043
17	16	20	230	174	46		1043
18	17	20	230	180	52		1044
19	18	20	230	186	58		1047
20	19	20	230	192	64		1050
21	20	20	230	198	70		1052
22	21	20	230	204	76		1055
23	22	20	230	210	82		1058
24	23	25	230	216	88		1054
25	24	30	230	222	94		1052

Table P8-2. Problem 8 Benchmark Case Results for VERA Computed Critical Boron Concentration for State Points 26-49 (Ref. 2)

Case	Hours	Power	Bank B	Bank C	Bank D	Flux Map	Computed Boron Concentration (ppm)
26	25	35	230	228	100		1050
27	26	40	230	230	106		1048
28	27	45	230	230	112		1046
29	28	50	230	230	118	Yes	1042
30	29	50	230	230	120		1042
31	30	55	230	230	128		1037
32	31	60	230	230	136		1032
33	32	65	230	230	144		1026
34	33	70	230	230	152		1019
35	34	75	230	230	160		1012
36	35	75	230	230	162		1007
37	36	75	230	230	164		1001
38	37	75	230	230	166		993
39	38	75	230	230	168		986
40	39	75	230	230	170		978
41	40	75	230	230	171		971
42	41	80	230	230	173		956
43	42	85	230	230	175		945
44	43	90	230	230	177		935
45	44	92	230	230	185		933
46	45	94	230	230	193		930
47	46	96	230	230	201		925
48	47	98	230	230	209		921
49	48	100	230	230	215	Yes	914

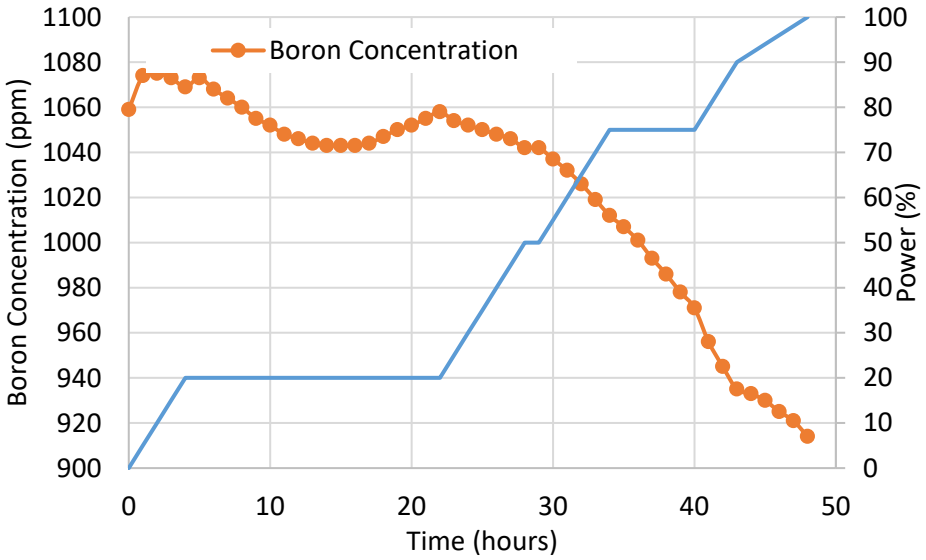

Figure P8-2. Critical Boron Concentration Plotted Against Reactor Power during the Specified Startup Procedure of Problem 8 (Ref. 2)

0.4263	0.7411	0.9316	0.8248	0.5290	0.9435	0.9914	0.8782
0.7411	0.8653	0.8188	0.9877	0.9464	1.1954	1.1788	1.0698
0.9316	0.8194	0.8535	0.9918	1.2047	1.2849	1.3327	1.0114
0.8248	0.9916	0.9929	1.0957	0.9917	1.2281	1.2529	0.8373
0.5290	0.9449	1.2091	0.9922	0.6287	0.8447	1.0798	
0.9435	1.1951	1.2845	1.2273	0.8439	0.9301	0.7071	
0.9914	1.1785	1.3276	1.2512	1.0752	0.7087		
0.8782	1.0736	1.0113	0.8394				

State Point 5, (20% Power, 1069 ppm Boron)

0.9169	0.9672	1.0799	1.0030	0.9726	1.0340	1.0913	0.8077
0.9672	1.0601	0.9655	1.1134	1.0440	1.1615	1.0689	0.9166
1.0799	0.9660	1.1233	1.0719	1.1798	1.1509	1.1063	0.8164
1.0030	1.1175	1.0729	1.1612	1.0535	1.1271	1.0381	0.6682
0.9726	1.0423	1.1840	1.0540	1.0759	0.8522	0.9259	
1.0340	1.1614	1.1509	1.1268	0.8517	0.8750	0.6213	
1.0913	1.0689	1.1026	1.0372	0.9224	0.6229		
0.8077	0.9198	0.8165	0.6700				

State Point 29, (50% Power, 1042 ppm Boron)

1.1107	1.0314	1.1105	1.0555	1.1468	1.0504	1.0418	0.7559
1.0314	1.1026	0.9846	1.1410	1.0802	1.1512	1.0143	0.8546
1.1105	0.9852	1.1291	1.0761	1.1787	1.1229	1.0517	0.7660
1.0555	1.1452	1.0772	1.1753	1.0815	1.1180	0.9918	0.6338
1.1468	1.0784	1.1830	1.0820	1.2366	0.8713	0.8986	
1.0504	1.1511	1.1229	1.1177	0.8709	0.8741	0.6118	
1.0418	1.0142	1.0481	0.9909	0.8953	0.6133		
0.7559	0.8575	0.7661	0.6355				

State Point 49, (100% Power, 914 ppm Boron)

Figure P8-3. Assembly Averaged Power Peaking Factors for Problem 8 VERA Benchmark Results, Showing State Points 5, 29 and 49

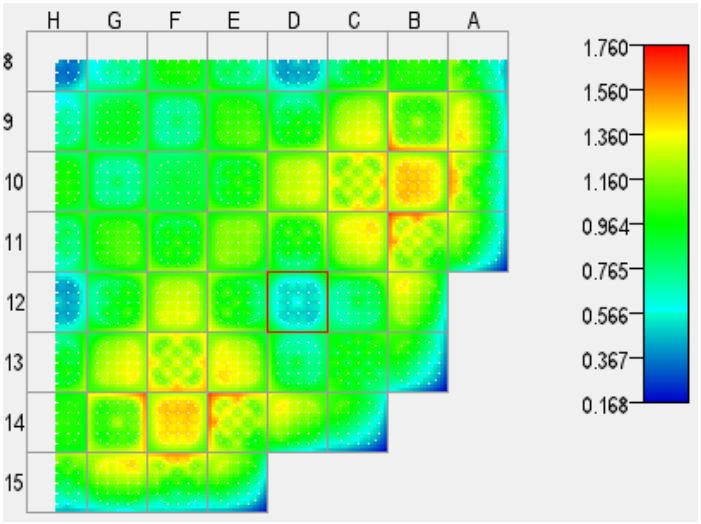

State Point 5, (20% Power, 1069 ppm Boron)

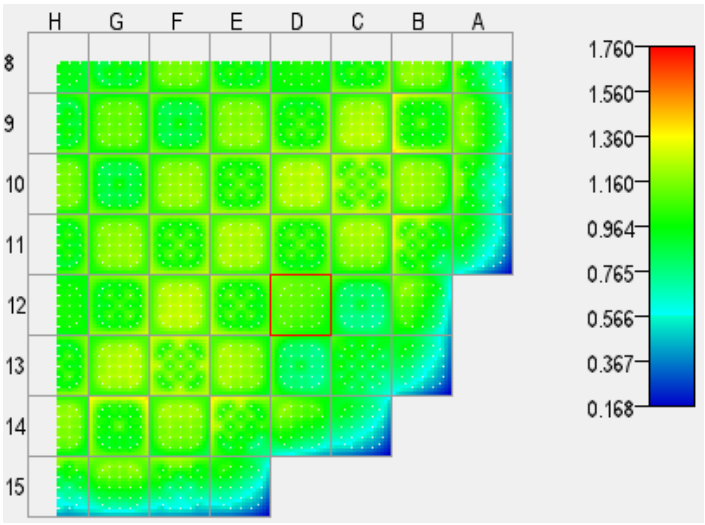

State Point 29, (50% Power, 1042 ppm Boron)

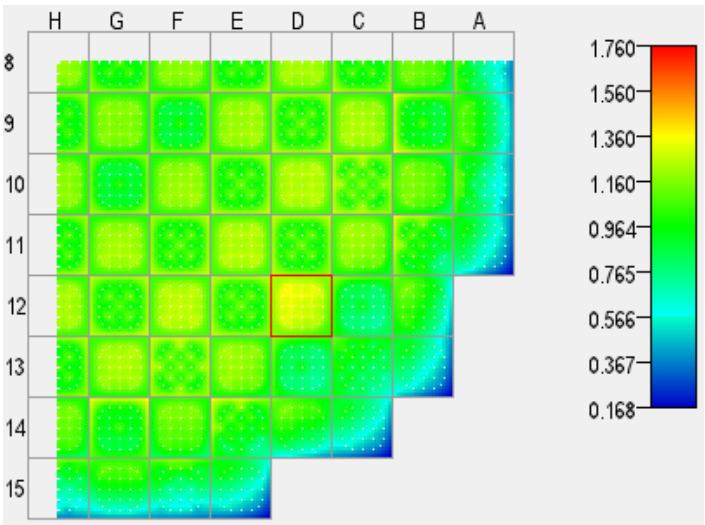

State Point 49, (100% Power, 914 ppm Boron)

Figure P8-4. Axially Averaged Pin Power Peaking Factors for Problem 8 VERA Benchmark Results, Showing State Points 5, 29 and 49

PROBLEM #9: PHYSICAL REACTOR DEPLETION

Description and Specification

This problem increases the required time scale to the length of a typical 18-month fuel cycle. This requires a significant number of time steps for accurate isotopic depletion and decay, as well as direct core follow simulations for substantial power maneuvers or periods of low power operation. The quality of the comparisons to measured data is partially dependent on how faithfully the actual operating history can be simulated, which can vary depending on the computational requirements of different M&S tools. (Ref. 2)

When generating these specifications, a typical industry benchmarking approach is applied using average operating conditions. Thermal-hydraulic feedback is required for at-power conditions, and the long time scale requires models for determining fuel temperatures as the fuel rod changes with temperature, irradiation, and burnup. The critical boron search capability is used to compare to the measured soluble boron concentrations when available, and the incore detector response capability provides direct comparison to incore flux map data that is typically produced every 4-6 weeks for standard plant core surveillance activities. Finally, the ability to predict cycle length and the fuel burnup distribution accurately is required before moving forward to Problem 10 through a restart capability. (Ref. 2)

The WBN1 reactor core geometry and rated operating characteristics are the same as provided in the previous whole reactor problems. For convenience, the relevant parameters and input for this problem are provided in Table P9-1. Steady-state depletion cases are required, beginning at beginning-of-cycle (BOC) and continuing to end-of-cycle (EOC).

Table P9-1. Problem 9 Input Specification (Ref. 2)

Input	Value
Rated Power (100%)	3411 MW
Rated Coolant Mass Flow (100%)	131.7 Mlbs/hr
Reactor Pressure	2250 psia
Cycle Length	441.0 EFPDs
EOC Exposure	16.939 GWd/MT
RCCA Overlap (steps withdrawn)	128

The operating power history for WBN1C1 was provided by the TVA. Observable is an initial startup extending approximately four months, five mid-cycle shutdowns, one of which lasted approximately 18 days, and an extended power coastdown at EOC for approximately seven weeks. The final model inputs for power level of Problem 9, based on the data from WBN1C1, are presented in Figure P9-1. These figure also includes the original operating data for reference. (Ref. 2)

Table P9-3 contains the benchmark specifications for Problem 9. The cases for which the input values are endpoints (not averages over the depletion interval) are shown with an asterisk. Table P9-2 contains estimates of the duration of each mid-cycle shutdown period. Such periods are not modeled in this benchmark. (Ref. 2)

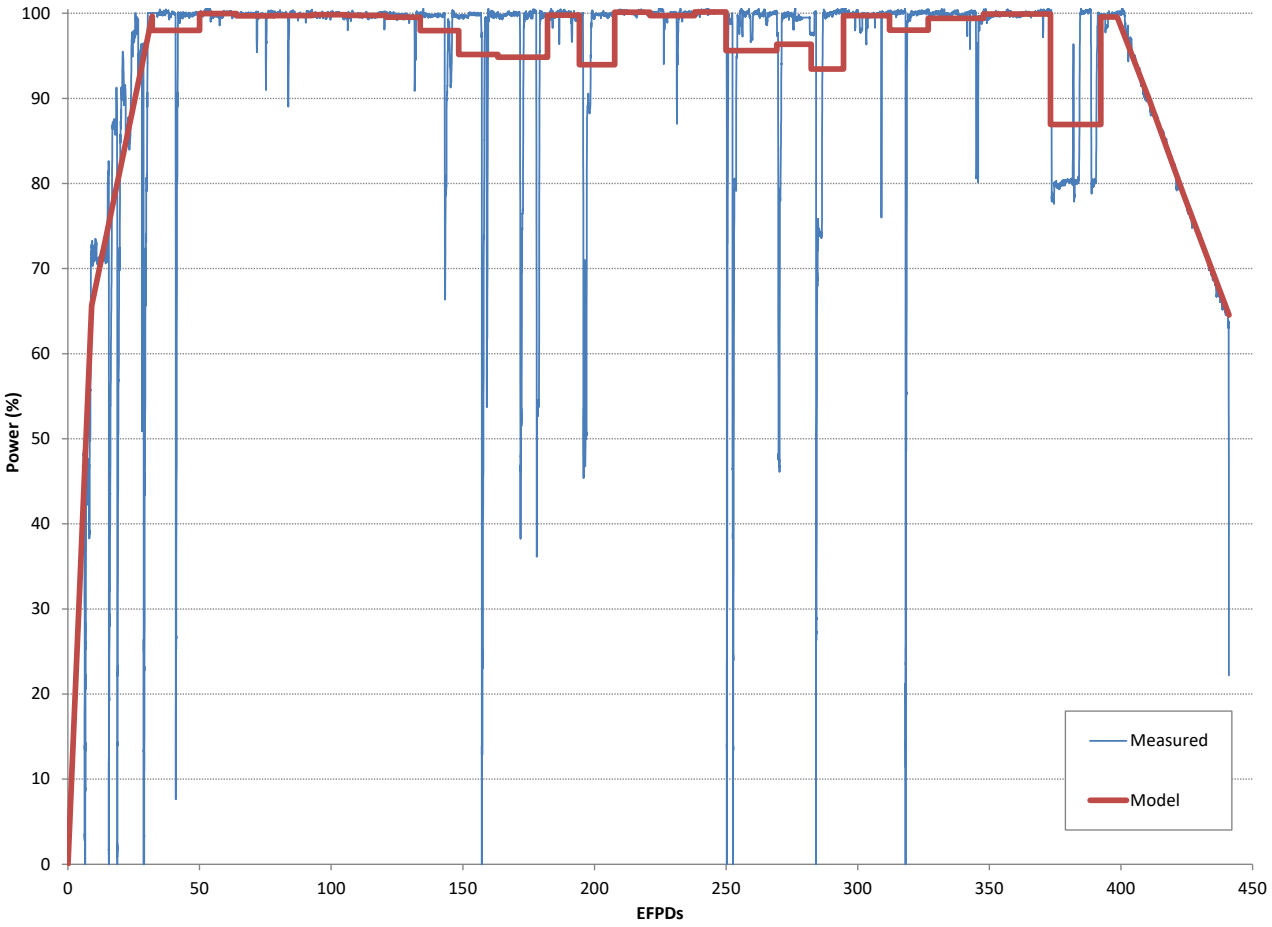

Figure P9-2. Problem 9 Model Input for Reactor Power (Ref. 2)

Table P9-2. Problem 9 Approximate Shutdown Durations (Ref. 2)

Event	EFPD	Duration (days)
1	6.5	3.4
2	15.5	4.8
3	18.8	1.6
4	28.8	0.8
5	28.9	4.7
6	157.2	18.0
7	250.2	1.6
8	252.6	3.7
9	284.1	9.1
10	318.2	1.5

Table P9-3. Problem 9 Cycle Depletion Specification (Ref. 2)

Case	EFPD	Cycle Exposure (GWd/MT)	Power (%)	Inlet Temp. (F)	Bank D Position (steps)
1	0.0	0.000	0.0	557.0	186
2*	9.0	0.346	65.7	557.6	192
3*	32.0	1.229	99.7	558.1	219
4	50.0	1.920	98.0	558.2	218
5	64.0	2.458	100.0	558.6	219
6	78.0	2.996	99.7	558.7	215
7	92.7	3.561	99.7	558.6	217
8	105.8	4.064	99.8	558.8	220
9	120.9	4.644	99.8	558.4	220
10	133.8	5.139	99.5	557.9	219
11	148.4	5.700	98.0	558.0	214
12	163.3	6.272	95.1	557.9	216
13	182.2	6.998	94.8	557.9	214
14	194.3	7.463	99.8	557.8	220
15	207.7	7.978	93.9	557.5	218
16	221.1	8.492	100.1	558.0	222
17	238.0	9.141	99.7	557.7	220
18	250.0	9.602	100.2	557.6	222
19	269.3	10.344	95.6	557.9	211
20	282.3	10.843	96.4	558.1	215
21	294.6	11.315	93.4	557.4	211
22	312.1	11.987	99.7	557.5	217
23	326.8	12.552	98.0	557.6	215
24	347.8	13.359	99.4	557.7	220
25	373.2	14.334	99.9	557.8	219
26	392.3	15.068	86.9	556.7	202
27	398.6	15.310	99.6	558.0	220
28*	410.7	15.775	89.9	557.1	224
29*	423.6	16.270	78.8	556.3	228
30*	441.0	16.939	64.5	554.9	230
Cycle Average			94.0	557.8	216.4

*The statepoint values are endpoints, not averages. If needed, the average values can be calculated or obtained from the author.

Benchmark Results

The results of the Problem 9 benchmark can be seen in Table P9-4, which shows the critical boron concentration as a function of cycle length. Values computed by VERA are compared against measured when available for any given burnup. It can be seen that VERA under-predicts critical boron concentration after 32 EFPD; before this no data is available. This is expressed graphically in Figure P9-2. As a result of this, VERA under-predicts the cycle length.

Table P9-4. Problem 9 Calculated Critical Boron Concentration for VERA Compared to Measured Data for State-points with Both Values (Ref. 2)

EFPD	Power (%)	VERA (ppm)	Measured (ppm)	Difference (ppm)
0	0	1296	-	-
9	65.7	1039	-	-
32	99.7	815	858	-43
50	98	792	843	-51
64	100	776	-	-
78	99.7	757	823	-66
92.7	99.7	736	-	-
105.8	99.8	715	790	-75
120.9	99.8	688	-	-
133.8	99.5	665	742	-77
148.4	98	639	-	-
163.3	95.1	617	-	-
182.2	94.8	578	-	-
194.3	99.8	538	592	-54
207.7	93.9	520	-	-
221.1	100.1	472	530	-58
238	99.7	427	-	-
250	100.2	395	458	-63
269.3	95.6	351	402	-51
282.3	96.4	316	370	-54
294.6	93.4	290	-	-
312.1	99.7	224	271	-47
326.8	98	181	235	-54
347.8	99.4	116	-	
373.2	99.9	35	95	-60
373.2	86.9	61	-	-
392.3	86.9	18	-	-
392.3	99.6	0	38	-38
398.6	99.6	0	9	-9
410.7	89.9	0	-	-
423.6	78.8	0	-	-
441	64.5	0	-	-

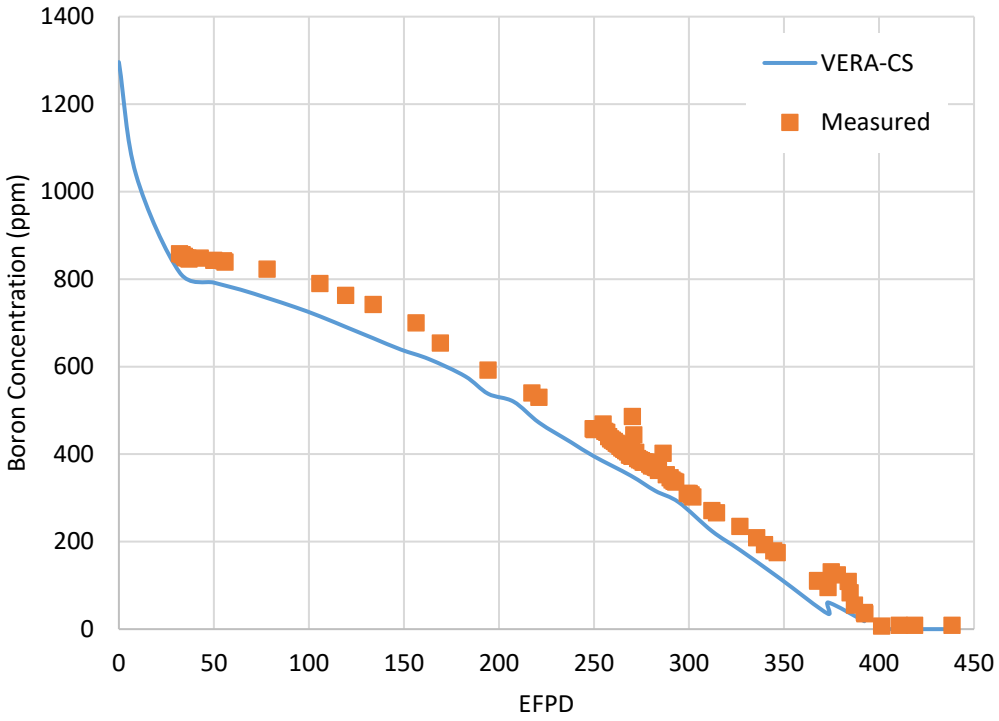

Figure P9-2. Problem 9 Measured and Computed Critical Boron Concentration (Ref. 2)

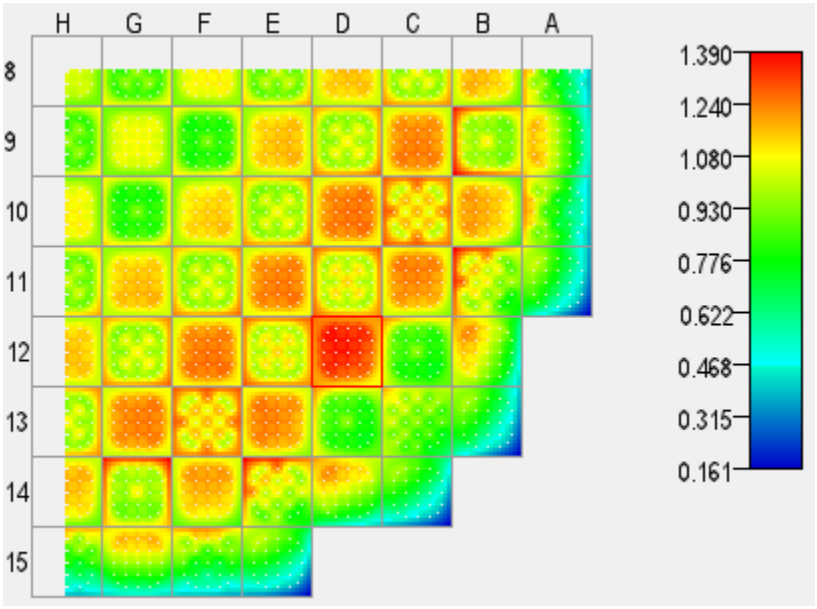

BOC, 0 EFPD

Figure P9-3. Axially-Averaged Pin Powers Computed using VERA for BOC, (Quadrant Symmetry)

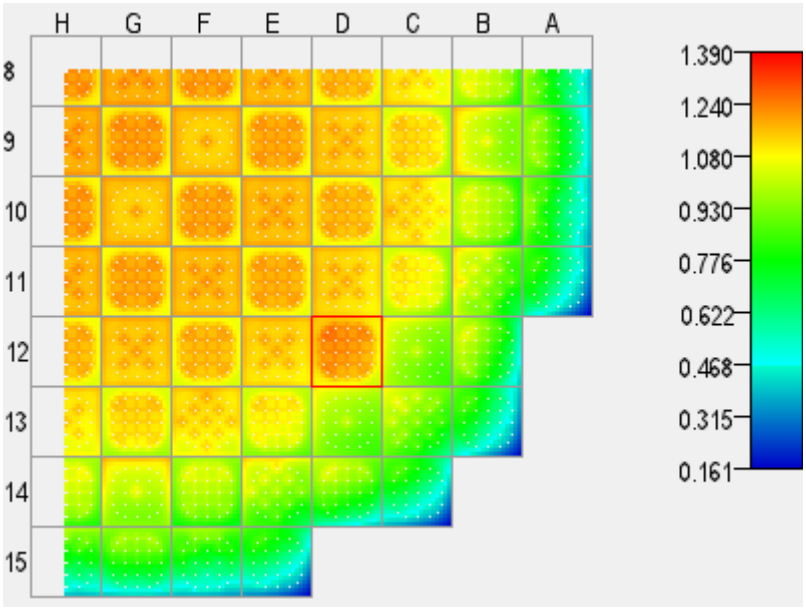

MOC, 221.1 EFPD

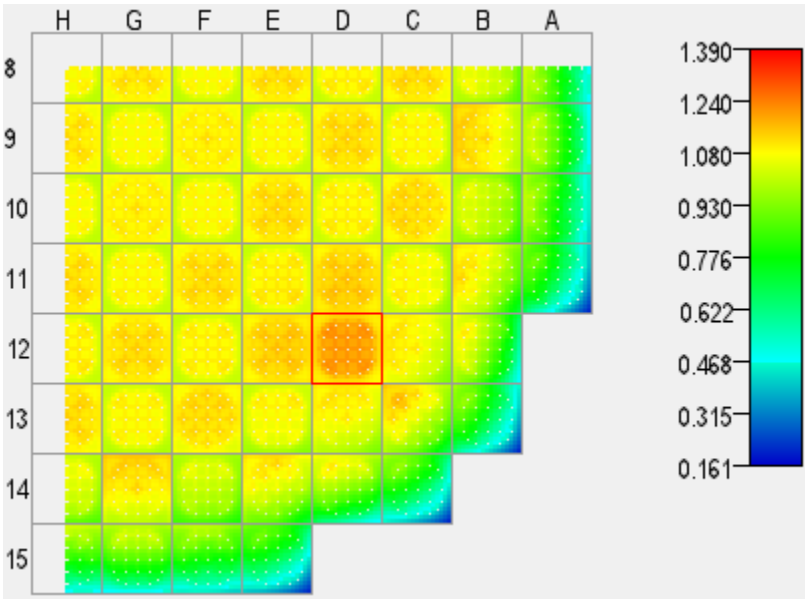

EOC, 441 EFPD

Figure P9-4. Axially-Averaged Pin Powers Computed using VERA for MOC and EOC, (Quadrant Symmetry)

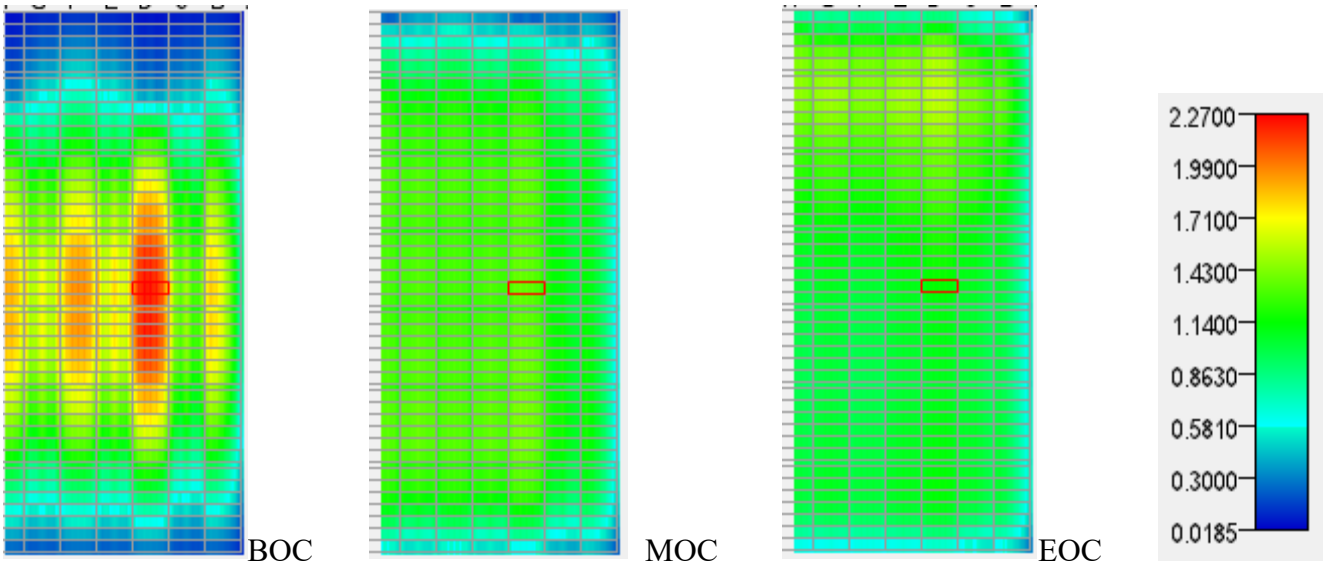

Figure P9-5. Axial Cross Section of the Simulated Reactor Showing Local Powers using VERA for BOC (0 EFPD), MOC (221.1 EFPD) and EOC (441 EFPD)

CONCLUSIONS

It can be concluded that VERA has the capability to model a wide range of nuclear power plant simulations, ranging from pin cells to full cycle depletions. Included below are several of the demonstrated capabilities of VERA, as well as issues that require further examination.

Demonstrated capabilities:

- Accurately predict local and averaged pin and assembly powers
- Accurately predict multiplication factor (K_{eff}) Eigen values
- 2D and 3D modeling
- 2D pin cell modeling, especially absent burnable absorbers
- 3D assembly modeling, especially absent burnable poison rods such as B_4C and Pyrex
- Calculate control rod and rod bank differential and integral worth, both full core and assembly level
- Calculate differential boron reactivity worth
- Coupled T/H and neutronic calculation using CTF and MPACT
- Perform reactor startup
- Perform full cycle depletions

Issues requiring further examination:

- ITC results obtained in Problem 5 cases 20 and 21 showed a computed ITC more negative than measured data. However, good agreement was found comparing the value to KENO-VI.
- The long-term boron letdown curve was less than measured values, resulting in under-predicted cycle length.

REFERENCES

1 Palmtag, S. and Godfrey, A., "VERA Common Input User Manual" CASL-U-2014-0014-002, February, 2015. http://www.casl.gov/docs/CASL-U-2014-0014-002.pdf.

2 Godfrey, A., "VERA Core Physics Benchmark Progression Problem Specifications, Revision 4" CAL-U-2012-0131-004, August, 2014. http://www.casl.gov/docs/CASL-U-2014-0014-002.pdf.

3 SCALE: A Comprehensive Modeling and Simulation Suite for Nuclear Safety Analysis and Design, ORNL/TM-2005/39, Version 6.1, June 2011. Available from Radiation Safety Information Computational Center at Oak Ridge National Laboratory as CCC-785.

4 D. F. Hollenbach, L. M. Petrie, and N. F. Landers, "KENO-VI: A General Quadratic Version of the KENO Program," Vol. II, Sect. F17 of SCALE: A Modular Code System for Performing Standardized Computer Analysis for Licensing Evaluation, NUREG/CR-0200, Rev. 7 (ORNL/NUREG/CR/CSD-2R7), 3 vols., April 2004. Available from the Radiation Safety Information Computational Center at Oak Ridge National Laboratory as CCC-545.

5 D. Griesheimer, et al., "MC21 v.6.0 – A Continuous-Energy Monte Carlo Particle Transport Code with Integrated Reactor Feedback Capabilities," Annals of Nuclear Energy, 82, 29 - 40 (2015).

6 Kelly, D. et al., "MC21/CTF and VERA Multiphysics Solutions to VERA Core Physics Benchmark Progression Problems 6 and 7," Presented at M&C 2017, April, 2017.